protease introduced into mouse embryonic stem (ES) cells were effective in restoring the function of TF proteins by removal of PTD, suggesting that directly delivered TF proteins may generally exert substantially enhanced functionality than presently considered.

2. Materials and methods

2.1. Cell culture

Mouse ES cells, 2TS22C, ZHBTc4, and Plat-E cells, were cultured according to the methods described by Masui et al. (2007), Niwa et al. (2000), and Morita et al. (2000), respectively.

2.2. Plasmid construction

An eleven arginine (11R) codon sequence was combined with cDNA of *Sox2* or *Oct3/4* to obtain 11RSox2 or 11ROct3/4 (Fig. 1A). Each construct was cloned into pPy vector with CAG-IB or CAG-IP to obtain pPyCAG-IB/11RSox2 or pPyCAG-IP/11ROct3/4. The TEV protease recognition sequence was inserted between the 11R sequence and *Sox2* or *Oct3/4* to obtain pPyCAG-IB/11RTEVRSox2 or pPyCAG-IP/11RTEVROct3/4 (Fig. 1C). The residual sequence after cleavage by TEV protease was ligated with the *Sox2* or *Oct3/4* sequence to obtain pPyCAG-IB/ΔTEVRSox2 or pPyCAG-IP/ΔTEVROct3/4 (Fig. 1B). These plasmids were generated through the following steps. For pPyCAG-IB/11RSox2, the 11R-Sox2 cDNA was amplified from pBRCAGIH/Sox2 using PCR with the primers 5′-11RSox2 (5′-ATACTCGAGCCACCATGGACGCAGGCGAAGGCGACGGGAGAATCTG-TACTATGGGTGATATCCAATGTATAACATGAT-3′ [XhoI site is underlined]) and 3′-Sox2 (5′-ACAGCGGCCGCTCACATGTGCGACAGGGG-CA-3′ [NotI site is underlined]). For pPyCAG-IB/ΔTEVRSox2, the ΔTEVRSox2 cDNA was amplified from pBRCAGIH/Sox2 using PCR with the primers 5′cutSox2 (5′-ATACTCGAGCCACCATGGGTGA-TATCCAATGTATAACATGAT-3′ [XhoI site is underlined]) and 3′-Sox2. For pPyCAG-IB/11RTEVRSox2, the 11RTEVRSox2 cDNA was amplified from pBRCAGIH/Sox2 using PCR with the primers 5′-11RTEVRSox2 (5′-ATACTCGAGCCACCATGGACGCAGGCGAAGG-CGACGGGAGAATCTGTACTTCCAGGGTGAGAATCTGTACTTCCAGG-GTGAGAATCTGTACTTCCAGGGTGAGAATCTGTACTATGGGTGATAT-CCAATGTATAACATGAT-3′ [XhoI site is underlined]) and 3′-Sox2. For pPyCAG-IP/11ROct3/4, the 11ROct3/4 cDNA was amplified from pBRCAGIH/Oct3/4 using PCR with the primers 5′-11ROct3/4 (5′-ATACTCGAGCCACCATGGACGCAGGCGAAGGCGACGGGAGAATCTG-TACTATGCCCACGTTCGACCAGGC-3′ [XhoI site is underlined]) and 3′-Oct3/4 (5′-ACAGCGGCCGCTCAGACATCAGAAGTAGAAA-3′ [NotI site is underlined]). For pPyCAG-IP/11RTEVROct3/4, the 11RTEVROct3/4 cDNA was amplified from pBRCAGIH/Oct3/4 using PCR with the primers 5′-11RTEVROct3/4 (5′-ATACTCGAGCC-ACCATGGACGCAGGCGAAGGCGACGGGAGAATCTGTACTTCCAGGG-TGAGAATCTGTACTTCCAGGGTGAGAATCTGTACTTCCAGGGTGAGA-ATCTGTACTATGCCCACGTTCGACCAGGC-3′ [XhoI site is under-lined]) and 3′-Oct3/4. For pPyCAG-IP/ΔTEVROct3/4, the ΔTEVROct3/4 cDNA was amplified from pBRCAGIH/Oct3/4 using PCR with the primers 5′-ΔTEVROct3/4 (5′-ATACTCGAG-CCACCATGCCCACGTTCGACCAGGC-3′ [XhoI site is underlined]) and 3′-Oct3/4. These cloning products were digested with XhoI and NotI.

Three different mutations in TEV protease cDNA were combined with drug resistance genes for hygromycin or histidinol. Six plasmid constructs, pMYsIH/TEV protease S219D mutant, pMYsIH/TEV protease S219P mutant, pMYsIH/TEV protease S219V mutant, pMYsIHisD/TEV protease S219D, pMYsIHisD/TEV protease S219P, and pMYsIHisD/TEV protease S219V mutant were generated through the following steps. For pMYsIH/TEV protease S219D and pMYsIHisD/TEV protease S219D, the TEV protease S219D cDNA was amplified from pRK603 (Addgene) using PCR with the primers 5′-S219D (5′-TTTGTCGACATGGGAGAAAGCTTGTTTAA-3′ [SalI site is underlined]) and 3′-S219D (5′-TTTGCGGCCGCATTAATTCATGAGTTGAGTC-3′ [NotI site is underlined]). For pMYsIH-IH/TEV protease S219P or S219V and pMYsIHisD/TEV protease S219P or S219V, the TEV protease S219P or S219V cDNA was amplified from pRK792 (Addgene) or pRK793 (Addgene) using PCR with the primers 5′-S219P (5′-TTTGTCGACGGTCATCATCATCATCATCA-3′ [SalI site is underlined]) and 3′-S219D (5′-TTTGCGGCCGCTTAGCGACGGCGACGACGAT-3′ [NotI site is underlined]).

2.3. Retroviral infection

Retroviral supernatant were prepared from Plat-E cells as described by Takahashi and Yamanaka (2006). Two days after infection, we initiated selection of 2TS22C using 0.1 mg/ml hygromycin (Invivogen) or ZHBTc4 using 3 mM histidinol (Sigma). The selection of clones was performed over a period of 2 weeks.

2.4. RT-PCR

The expression of TEV protease gene and the pluripotency marker genes *Oct3/4* and *Nanog* was determined by RT-PCR. Total RNA was extracted using Isogen (Nippon Gene) as described by the manufacturer and then treated with High-Capacity RNA-to-cDNA kit (AB gene) to generate cDNA. Then PCR amplification was performed for the three types of TEV protease mutant gene. PCR cycles were as follows: 95 °C for 5 min, 95 °C for 30 s, annealing temperature for 30 s, 72 °C for 1 min (25–30 cycles), and 72 °C for 3 min. The RT-PCR products were analyzed using 1% agarose gel electrophoresis and visualized with ethidium bromide. Primers used in this study are *TEVprotease* (S219V and S219P) (5′-CACTCAGCATCGAATTTCACCAA-3′ and 5′-GCTGAAAAGGCTCTTCAGGTTTC-3′), *TEVprotease* (S219D) (5′-TACA-CTCAGCATCGAATTTCACCAA-3′ and 5′-AAAAGGCTCTTCAGGTTT-GTCCA-3′), *GAPDH* (5′-TGAAGGTCGGTGTGAACGGATTTGGC-3′ and 5′-CATGTAGGCCATGAGGTCCACCA-3′), and *Nanog* (5′-GTAGC-TGTCTTCAGACACTCC-3′ and 5′-AATTAGAGCTATGCAGAGAAA-3′).

2.5. TF rescue experiment

Sox2 and *Oct3/4* repression was induced by the addition of tetracycline (Tc) (1 μg/ml) to 2TS22C and ZHBTc4 culture media (Masui et al., 2007; Niwa et al., 2000). Plasmids containing various forms of TFs (Fig. 1) were introduced to these cells using lipofectamin 2000 (Invitrogen) according to the manufacturer's recommendations. Cells were replated in Tc^+ or Tc^- media and selected for 2TS22C cells using 10 μg/ml blasticidin S (Invivogen) for 14 days or for ZHBTc4 cells using 1 μg/ml puromycin (Invivogen) for 10 days. Colonies identified by Leishman (Sigma, St Louis, MO) staining were counted. The rescue index of a given cDNA was determined by the ratio of colonies in Tc^+ to those in Tc^- media after subtracting the ratio of empty vector (background), which was then normalized by the ratio of *Sox2* or *Oct3/4* expression vector (positive control).

3. Results

3.1. PTDs interfere with the function of Sox2 and Oct3/4

To investigate whether Sox2 fused with PTD retained its normal function, we employed a functional complementation system based on the drug-inducible Sox2 knockout ES cells, 2TS22C. Here, endogenous *Sox2* is repressed in 2TS22C upon addition of Tc, which leads to differentiation of these cells and to reduction in colony-forming capacity (reflected in colony number). The number of

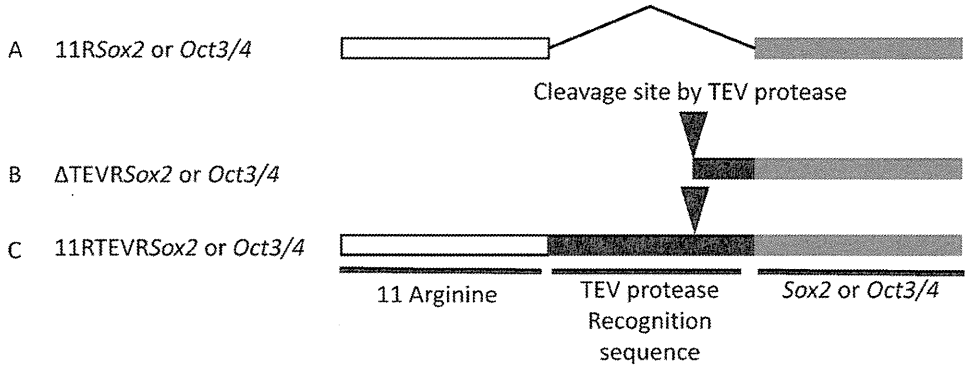

Fig. 1. Expression vectors used in the rescue experiments. (A) An eleven arginine (11R) sequence codon was ligated with *Sox2* or *Oct3/4* cDNA, (B) the residual sequence after cleavage of TEV protease was ligated with *Sox2* or *Oct3/4* cDNA, and (C) a TEV protease recognition sequence was inserted between the 11R sequence and *Sox2* or *Oct3/4* cDNA.

colonies increases only when exogenously introduced *Sox2* is functional (Masui et al., 2007). The normalized ratio of colony number, termed rescue index, reflects the relative activity of exogenous *Sox2*. When 11R or VP22 as a PTD was fused with Sox2, the rescue indices were greatly reduced compared with wild-type Sox2, suggesting that PTD interfered with the function of Sox2 (Table 1). Conversely, Sox2 fused with the residual sequence of the TEV protease recognition site showed an enhanced rescue index, suggesting that cleavage between PTD and Sox2 by TEV protease will be able to restore the function.

Next, to examine whether PTD disturbs the function of another TF, we assayed Oct3/4 fused with PTD in ZHBTc4, which represses endogenous *Oct3/4* expression in Tc^+ and loses colony-forming capacity. As in the case of Sox2, Oct3/4 fusion with 11R greatly reduced its function, whereas in the case of Oct3/4 without 11R (with the residual sequence of the TEV protease recognition site), the function was restored substantially (Table 1). These results suggest that the addition of PTD to TFs compromises the function of TFs, whereas intracellular removal of PTD by TEV protease restores the function.

3.2. Expression of TEV protease in ES cells does not compromise pluripotent stem cell specific gene expression

Wild-type TEV protease is known to be unstable because of its self-cleaving activity. More stable and efficient TEV protease mutants have been developed (Kapust et al., 2001), which are reported to be active in a variety of species including *E. coli* (Kapust and Waugh, 2000), yeast (Rigaut et al., 1999), *Drosophila* (Pauli et al., 2008), *Xenopus* (Wawersik et al., 2005) and rat (Wehr et al., 2006). To establish mouse ES cells expressing TEV protease, we infected mouse ES cells (2TS22C or ZHBTc4) with retroviruses carrying three types of TEV protease mutant (TEV-S219D, TEV-S219P or TEV-S219V). We confirmed that these ES cells expressed transgenes for TEV protease mutants (Fig. 2A). We then checked for the expression level of *Nanog*, marker gene for pluripotency, and found that they were maintained at almost the same level as the wild-type (Fig. 2B), suggesting that TEV protease did not cleave endogenous proteins necessary to maintain cellular identity.

Table 1
PTDs interfere with TF function.

Vectors	Tc^+ (Sox2 null)	Tc^-	Rescue index
(A) 2TS22C			
pPyCAGIB	22	344	0
pPyCAGSox2IB	270	286	1.0
pPyCAGIB/VP22Sox2	49	466	0.07
pPyCAGIB/11RSox2	57	436	0.09
pPyCAGIB/Δ TEVR-Sox2	162	258	0.63
Vectors	**Tc^+ (Oct3/4 null)**	**Tc^-**	**Rescue index**
(B) ZHBTc4			
pPyCAGIP	3	603	0
pPyCAGOct3/4IP	256	285	1.0
pPyCAGIP/11ROct3/4	8	216	0.03
pPyCAGIP/Δ TEVR-Oct3/4	248	298	0.93

The results of assay in 2TS22C (A) and ZHBTc4 (B). Colony numbers are shown in Tc^+ and Tc^- column.

3.3. TEV protease-expressing ES cells can restore the function of Sox2 fused with PTD

To address whether TEV protease can function in ES cells and contribute to restoring the function of TF by removing PTD, we introduced 11RSox2, ΔTEVRSox2, or 11RTEVRSox2 (containing TEV protease recognition site between 11R and Sox2) into wild-type 2TS22C or 2TS22C expressing the TEV protease mutants (2TS22C-TEVS219D, 2TS22C-TEVS219P or 2TS22C-TEVS219V). As

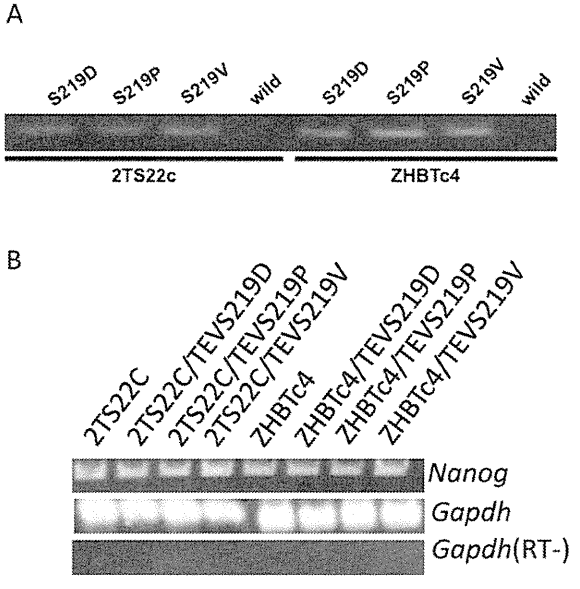

Fig. 2. Expression of TEV protease in ES cells does not compromise pluripotent stem cell specific gene expression. (A) RT-PCR analysis to confirm expression of transgenes for TEV protease mutants (S219D, S219P, S219V) and (B) RT-PCR analysis for *Nanog* in the ES cells.

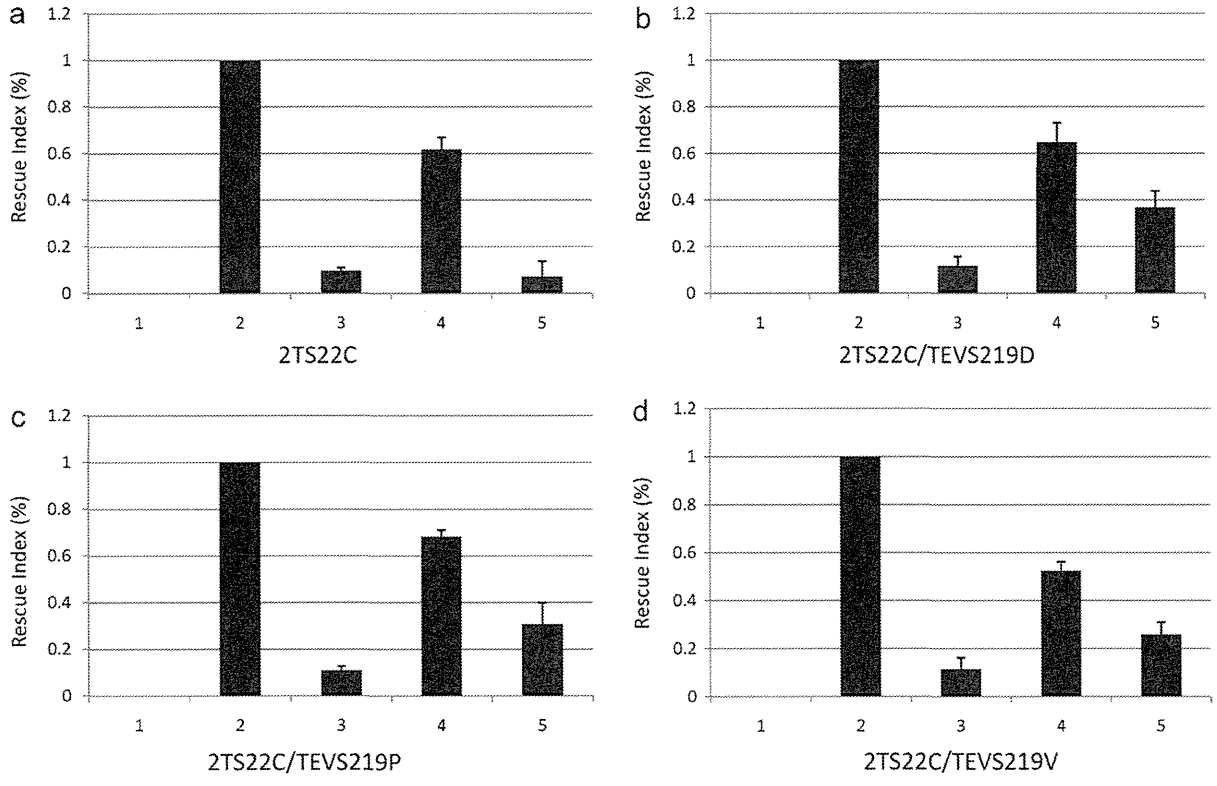

Fig. 3. TEV protease-expressing ES cells can restore the function of Sox2 fused with PTD. 1, pPyCAG-IB, empty vector; 2, pPyCAGSox2-IB; 3, pPyCAG-IB/11RSox2, 11R-containing Sox2; 4, pPyCAG-IB/ΔTEVRSox2, truncated form of Sox2 with residual fusion protein; 5, pPyCAG-IB/11RTEVRSox2, 11R-TEV recognition sequence-Sox2.

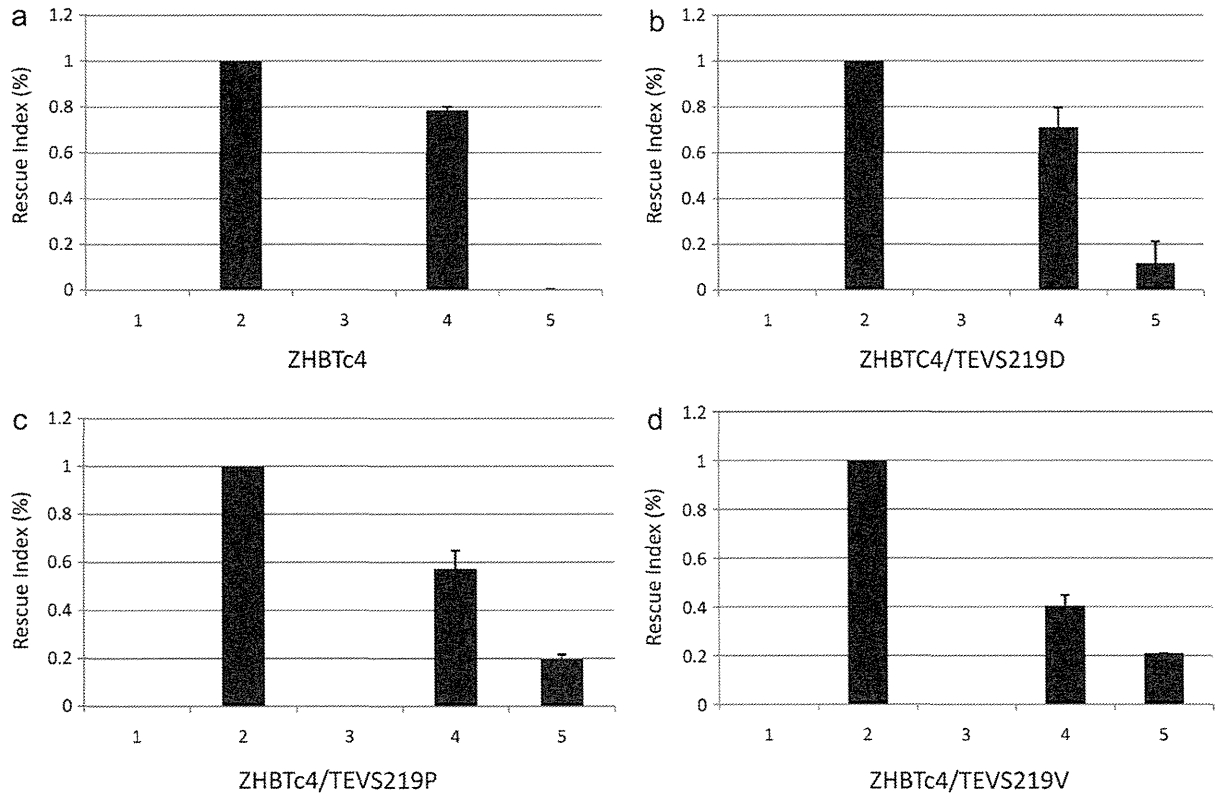

Fig. 4. TEV protease-expressing ES cells can restore the function of Oct3/4 fused with PTD. 1, pPyCAG-IP, empty vector; 2, pPyCAGOct3/4-IP; 3, pPyCAG-IP/11ROct3/4, 11R-containing Oct3/4; 4, pPyCAG-IP/ΔTEVROct3/4, truncated form of Oct3/4 with residual fusion protein; 5, pPyCAG-IP/11RTEVROct3/4, 11R-TEV recognition sequence-Oct3/4.

expected, the rescue index of 11RSox2 was greatly reduced (Fig. 3a–d, lane 3). In contrast, 11RTEVRSox2 substantially enhanced rescue index to a level comparable to that of ΔTEVRSox2 (Fig. 3b–d, lanes 4 and 5). This restoration of function was due to the activity of TEV protease, since no enhancement was observed in 2TS22C without the TEV protease transgene (Fig. 3a, lanes 4 and 5). These results indicate that the TEV protease cleaved 11RTEVRSox2 protein to remove PTD, which restored Sox2 function. The efficacy of the three TEV protease mutants was comparable.

3.4. TEV protease-expressing ES cells can restore the function of Oct3/4 fused with PTD

To determine whether the function of another TF can be recovered by removing the PTD, we introduced 11ROct3/4, ΔTEVROct3/4 or 11RTEVROct3/4 into wild-type ZHBTc4 or ZHBTc4 expressing the TEV protease mutants (ZHBTc4-TEVS219D, ZHBTc4-TEVS219P and ZHBTc4-TEVS219V). As expected, the rescue index of 11ROct3/4 was greatly reduced (Fig. 4a–d, lane 3). In contrast, 11RTEVROct3/4 substantially enhanced the rescue index to a level comparable to that of ΔTEVROct3/4 (Fig. 4b–d, lanes 4 and 5). This functional restoration was due to the activity of TEV protease, as no enhancement was observed in ZHBTc4 without the TEV protease transgene (Fig. 4a, lanes 4 and 5). These results indicate that TEV protease cleaved 11RTEVROct3/4 protein to remove PTD, which restored Oct3/4 function. The efficacy of the three TEV protease mutants was comparable.

Collectively, these results suggest that a PTD interferes with the function of TFs, which can be restored by intracellular removal of PTD by TEV protease.

4. Discussion

To date, there are three approaches to circumvent insertional mutagenesis in cellular induction experiments. (i) In a non-integration type DNA-based approach such as an episomal vector, occasional integration into the genome has been observed (Okita et al., 2008). Thus it is desirable to avoid introducing exogenous DNA into the cell. (ii) In an RNA-based approach, such as mRNA transfection (Warren et al., 2010), expression level may not be strong and continuous enough to induce global change in transcriptional profile. This may limit usefulness to general applications. In fact, a number of mRNA transfections are required for induction of iPS cells (Warren et al., 2010). Conversely, in Sendai virus (SeV), the RNA virus that does not integrate with the genome, transgene expression is known to be strong and continuous because SeV replicates in the cell (Li et al., 2000). Although it is known that SeV in the cells can be eliminated by using temperature-sensitive replication mutants of SeV (Inoue et al., 2003), for clinical use it will be difficult to achieve complete elimination from all the cells. This may result in unexpected effects of transgene TFs a long time after cell replacement therapy. (iii) A protein-based approach such as protein transduction, does not produce residual exogenous TFs upon withdrawal from the medium. In addition, unlike mRNA transfection, protein transduction does not require a transfection reagent, which is generally toxic to cells, so that TFs can be continuously added to the medium at a high concentration, enabling strong and continuous expression. However, their use has been hampered by the interference of PTDs with the function of TFs (Ye et al., 2002). In this study, we demonstrated that intracellular removal of PTD indeed restored the function of TFs using TEV protease as an example of this strategy. The activity of TEV protease was probably sufficient for processing most TFs, since quite a high level of exogenous Sox2 or Oct3/4 is known to be required for rescuing the repression of endogenous counterparts in ES cells. In future, it is conceivable that combination of PTD-TEVR-TFs introduced by protein transduction with TEV protease expressed by an RNA-based system (e.g., SeV) may achieve efficient cellular induction. In addition, this may reduce concern for any unexpected effect of expression of residual TFs (compared with all TFs being introduced by SeV), and may considerably reduce safety verification steps for clinical use.

In summary, we demonstrated that removal of PTD fused with Sox2 or Oct3/4 within ES cells restored protein function. This suggests that if PTD is removed from cells, directly delivered TF proteins, in general, may be able to exert substantially enhanced function than presently considered. This may enable induction of most cell types by protein transduction, and TEV protease may be a useful tool for this approach.

Funding

This work was supported in part by Grants-in-Aid for Scientific Research from the Ministry of Health, Labor, and Welfare of Japan.

Acknowledgments

We are grateful to Dr. Barbara Lee Smith Pierce (University of Maryland University College) for editorial work in the preparation of this manuscript.

References

Davis, R.L., Weintraub, H., Lassar, A.B., 1987. Expression of a single transfected cDNA converts fibroblasts to myoblasts. Cell 51, 987–1000.
Derossi, D., Calvet, S., Trembleau, A., Brunissen, A., Chassaing, G., Prochiantz, A., 1996. Cell internalization of the third helix of the Antennapedia homeodomain is receptor-independent. J. Biol. Chem. 271, 18188–18193.
Dougherty, W.G., Carrington, J.C., Cary, S.M., Parks, T.D., 1988. Biochemical and mutational analysis of a plant virus polyprotein cleavage site. EMBO J. 7, 1281–1287.
Feng, R., Desbordes, S.C., Xie, H., Tillo, E.S., Pixley, F., Stanley, E.R., Graf, T., 2008. PU.1 and C/EBPalpha/beta convert fibroblasts into macrophage-like cells. Proc. Natl. Acad. Sci. U.S.A. 105, 6057–6062.
Frankel, A.D., Pabo, C.O., 1988. Cellular uptake of the tat protein from human immunodeficiency virus. Cell 55, 1189–1193.
Hanna, J., Wernig, M., Markoulaki, S., Sun, C.W., Meissner, A., Cassady, J.P., Beard, C., Brambrink, T., Wu, L.C., Townes, T.M., Jaenisch, R., 2007. Treatment of sickle cell anemia mouse model with iPS cells generated from autologous skin. Science 318, 1920–1923.
Ieda, M., Fu, J.D., Delgado-Olguin, P., Vedantham, V., Hayashi, Y., Bruneau, B.G., Srivastava, D., 2010. Direct reprogramming of fibroblasts into functional cardiomyocytes by defined factors. Cell 142, 375–386.
Inoue, M., Tokusumi, Y., Ban, H., Kanaya, T., Tokusumi, T., Nagai, Y., Iida, A., Hasegawa, M., 2003. Nontransmissible virus-like particle formation by F-deficient sendai virus is temperature sensitive and reduced by mutations in M and HN proteins. J. Virol. 77, 3238–3246.
Kapust, R.B., Tozser, J., Fox, J.D., Anderson, D.E., Cherry, S., Copeland, T.D., Waugh, D.S., 2001. Tobacco etch virus protease: mechanism of autolysis and rational design of stable mutants with wild-type catalytic proficiency. Protein Eng 14, 993–1000.
Kapust, R.B., Waugh, D.S., 2000. Controlled intracellular processing of fusion proteins by TEV protease. Protein Expr Purif 19, 312–318.
Kim, D., Kim, C.H., Moon, J.I., Chung, Y.G., Chang, M.Y., Han, B.S., Ko, S., Yang, E., Cha, K.Y., Lanza, R., Kim, K.S., 2009. Generation of human induced pluripotent stem cells by direct delivery of reprogramming proteins. Cell Stem Cell 4, 472–476.
Li, H.O., Zhu, Y.F., Asakawa, M., Kuma, H., Hirata, T., Ueda, Y., Lee, Y.S., Fukumura, M., Iida, A., Kato, A., Nagai, Y., Hasegawa, M., 2000. A cytoplasmic RNA vector derived from nontransmissible Sendai virus with efficient gene transfer and expression. J. Virol. 74, 6564–6569.
Masui, S., Nakatake, Y., Toyooka, Y., Shimosato, D., Yagi, R., Takahashi, K., Okochi, H., Okuda, A., Matoba, R., Sharov, A.A., Ko, M.S., Niwa, H., 2007. Pluripotency governed by Sox2 via regulation of Oct3/4 expression in mouse embryonic stem cells. Nat. Cell Biol. 9, 625–635.
Matsushita, M., Tomizawa, K., Moriwaki, A., Li, S.T., Terada, H., Matsui, H., 2001. A high-efficiency protein transduction system demonstrating the role of PKA in long-lasting long-term potentiation. J. Neurosci. 21, 6000–6007.
Morita, S., Kojima, T., Kitamura, T., 2000. Plat-E: an efficient and stable system for transient packaging of retroviruses. Gene Ther. 7, 1063–1066.
Niwa, H., Miyazaki, J., Smith, A.G., 2000. Quantitative expression of Oct-3/4 defines differentiation, dedifferentiation or self-renewal of ES cells. Nat. Genet. 24, 372–376.
Okita, K., Ichisaka, T., Yamanaka, S., 2007. Generation of germline-competent induced pluripotent stem cells. Nature 448, 313–317.

Okita, K., Nakagawa, M., Hyenjong, H., Ichisaka, T., Yamanaka, S., 2008. Generation of mouse induced pluripotent stem cells without viral vectors. Science 322, 949–953.

Pauli, A., Althoff, F., Oliveira, R.A., Heidmann, S., Schuldiner, O., Lehner, C.F., Dickson, B.J., Nasmyth, K., 2008. Cell-type-specific TEV protease cleavage reveals cohesin functions in Drosophila neurons. Dev Cell 14, 239–251.

Phelan, A., Elliott, G., O'Hare, P., 1998. Intercellular delivery of functional p53 by the herpesvirus protein VP22. Nat. Biotechnol. 16, 440–443.

Rigaut, G., Shevchenko, A., Rutz, B., Wilm, M., Mann, M., Seraphin, B., 1999. A generic protein purification method for protein complex characterization and proteome exploration. Nat Biotechnol 17, 1030–1032.

Takahashi, K., Yamanaka, S., 2006. Induction of pluripotent stem cells from mouse embryonic and adult fibroblast cultures by defined factors. Cell 126, 663–676.

Takenobu, T., Tomizawa, K., Matsushita, M., Li, S.T., Moriwaki, A., Lu, Y.F., Matsui, H., 2002. Development of p53 protein transduction therapy using membrane-permeable peptides and the application to oral cancer cells. Mol. Cancer Ther. 1, 1043–1049.

Vierbuchen, T., Ostermeier, A., Pang, Z.P., Kokubu, Y., Sudhof, T.C., Wernig, M., 2010. Direct conversion of fibroblasts to functional neurons by defined factors. Nature 463, 1035–1041.

Warren, L., Manos, P.D., Ahfeldt, T., Loh, Y.H., Li, H., Lau, F., Ebina, W., Mandal, P.K., Smith, Z.D., Meissner, A., Daley, G.Q., Brack, A.S., Collins, J.J., Cowan, C., Schlaeger, T.M., Rossi, D.J., 2010. Highly efficient reprogramming to pluripotency and directed differentiation of human cells with synthetic modified mRNA. Cell Stem Cell 7, 618–630.

Wawersik, S., Evola, C., Whitman, M., 2005. Conditional BMP inhibition in Xenopus reveals stage-specific roles for BMPs in neural and neural crest induction. Dev Biol 277, 425–442.

Wender, P.A., Mitchell, D.J., Pattabiraman, K., Pelkey, E.T., Steinman, L., Rothbard, J.B., 2000. The design, synthesis, and evaluation of molecules that enable or enhance cellular uptake: peptoid molecular transporters. Proc. Natl. Acad. Sci. U.S.A. 97, 13003–13008.

Wernig, M., Zhao, J.P., Pruszak, J., Hedlund, E., Fu, D., Soldner, F., Broccoli, V., Constantine-Paton, M., Isacson, O., Jaenisch, R., 2008. Neurons derived from reprogrammed fibroblasts functionally integrate into the fetal brain and improve symptoms of rats with Parkinson's disease. Proc. Natl. Acad. Sci. U.S.A. 105, 5856–5861.

Wehr, M.C., Laage, R., Bolz, U., Fischer, T.M., Grunewald, S., Scheek, S., Bach, A., Nave, K.A., Rossner, M.J., 2006. Monitoring regulated protein-protein interactions using split TEV. Nat Methods 3, 985–993.

Ye, D., Xu, D., Singer, A.U., Juliano, R.L., 2002. Evaluation of strategies for the intracellular delivery of proteins. Pharm. Res. 19, 1302–1309.

Zhou, Q., Brown, J., Kanarek, A., Rajagopal, J., Melton, D.A., 2008. In vivo reprogramming of adult pancreatic exocrine cells to beta-cells. Nature 455, 627–632.

厚生労働科学研究費補助金

第3次対がん総合戦略研究事業

幹細胞制御によるがん治療法開発のための基盤研究

平成21-23年度　　**総合・分担研究報告書**

研究代表者　落谷　孝広

平成24（2011）年5月

（2／3冊）

Journal of Reproduction and Development, Vol. 57, No. 5, 2011

—Original Article—

The *Dnmt3b* Splice Variant is Specifically Expressed in *In Vitro*-manipulated Blastocysts and Their Derivative ES Cells

Takuro HORII[1], Isao SUETAKE[2], Eikichi YANAGISAWA[1], Sumiyo MORITA[1], Mika KIMURA[1], Yasumitsu NAGAO[3], Hiroshi IMAI[4], Shoji TAJIMA[2] and Izuho HATADA[1]

[1]Laboratory of Genome Science, Biosignal Genome Resource Center, Institute for Molecular and Cellular Regulation, Gunma University, Gunma 371-8512, [2]Laboratory of Epigenetics, Institute for Protein Research, Osaka University, Osaka 565-0871, [3]Medical Research Center, Jichi Medical University, Tochigi 329-0498 and [4]Laboratory of Reproductive Biology, Graduate School of Agriculture, Kyoto University, Kyoto 606-8502, Japan

Abstract. Manipulation of preimplantation embryos *in vitro*, such as *in vitro* fertilization (IVF), *in vitro* culture (IVC), intracytoplasmic sperm injection (ICSI), somatic cell nuclear transfer (SCNT) and other assisted reproduction technologies (ART), has contributed to the development of infertility treatment and new animal reproduction methods. However, such embryos often exhibit abnormal DNA methylation patterns in imprinted genes and centromeric satellite repeats. These DNA methylation patterns are established and maintained by three DNA methyltransferases: Dnmt1, Dnmt3a and Dnmt3b. Dnmt3b is responsible for the creation of methylation patterns during the early stage of embryogenesis and consists of many alternative splice variants that affect methylation activity; nevertheless, the roles of these variants have not yet been identified. In this study, we found an alternatively spliced variant of *Dnmt3b* lacking exon 6 (*Dnmt3bΔ6*) that is specific to mouse IVC embryos. *Dnmt3bΔ6* also showed prominent expression in embryonic stem (ES) cells derived from *in vitro* manipulated embryos. Interestingly, IVC blastocysts were hypomethylated in centromeric satellite repeat regions that could be susceptible to methylation by Dnmt3b. *In vitro* methylation activity assays showed that Dnmt3bΔ6 had lower activity than normal Dnmt3b. Our findings suggest that Dnmt3bΔ6 could induce a hypomethylation status especially in *in vitro* manipulated embryos.
Key words: DNA methylation, Dnmt3b, *In vitro* culture

(J. Reprod. Dev. 57: 579–585, 2011)

The 5th position cytosine residues in CpG sequences are often methylated in vertebrate genomic DNA [1]. DNA methylation plays an essential role in the normal development of mammalian embryos by regulating gene expression through genomic imprinting, X chromosome inactivation and genomic stability [2–6]. In vertebrates, two types of DNA methyltransferase activity have been reported, the *de novo* and maintenance types. In mice, *de novo*-type DNA methylation activity creates gene-specific methylation patterns during the implantation stage of embryogenesis, while maintenance-type activity ensures clonal transmission of lineage-specific methylation patterns during replication. Dnmt1 is responsible for the latter activity. On the other hand, two DNA methyltransferases, Dnmt3a and Dnmt3b, are responsible for creation of methylation patterns during the early stages of embryogenesis [7, 8] and have been shown to possess *de novo*-type DNA methylation activity *in vitro* [9–12]. Recent studies have shown that Dnmts function in cooperation with each other to facilitate DNA methylation in both humans and mice [13–15].

In mice, Dnmt3b is the major *de novo* DNA methyltransferase in E (embryonic stage) 4.5–7.5 embryos, and its expression is down-regulated after midgestation [8, 16]. Disruption of Dnmt3b results in embryonic lethality at E13.5 and hypomethylation of centromeric minor satellite repeats [8]. In humans, DNMT3B mutations have been shown to cause ICF (immunodeficiency, chromosomal instability, and facial anomalies) syndrome [8, 17, 18]. Dnmt3b contains a C-terminal catalytic domain and a N-terminal regulatory domain including the PWWP domain and consists of more than 16 alternative splice variants [7, 19–22]. Among these variants, both Dnmt3b1 and Dnmt3b2 contain all of the highly conserved motifs (I, IV, VI, VIII, IX and X) in their catalytic domains. In contrast, Dnmt3b3 and Dnmt3b6, lacking motifs VII and VIII and nine amino acids of motif IX [19], are catalytically inactive both *in vitro* [9] and *in vivo* [23]. On the other hand, the splicing variant of the regulatory domain, human DNMT3BΔ5 (the same variant as mouse Dnmt3bΔ6), which lacks exon 5 (exon 6) adjacent to the PWWP domain, was recently reported to be upregulated in cancer cell lines that often show hypomethylation in centromeric repeated sequences [24]. Gopalakrishnan *et al.* indicated that this splicing region is responsible for DNA binding activity [24]; however, the role of this region has not yet been fully investigated. Interestingly, forced expression of DNMT3BΔ5 results in hypomethylation of centromeric and pericentromeric repeated sequences [24]. Similarly, forced expression of human specific DNMT3B4, which lacks a catalytic domain, induced DNA demethylation on satellite 2 in pericentromeric DNA [25]. These reports indicate that Dnmt3b variants have complicated roles in maintenance of DNA methylation status.

As is generally known, *in vitro* embryo manipulation technologies such as IVC, ICSI and SCNT have contributed to the

Received: October 22, 2010
Accepted: April 27, 2011
Published online in J-STAGE: June 10, 2011

Correspondence: I Hatada (e-mail: hatada@gunma-u.ac.jp)

development of infertility treatments and animal reproduction techniques. However, it has been reported that *in vitro* manipulated embryos often show abnormal DNA methylation patterns in differentially methylated regions (DMRs) of imprinted genes [26–29]. Moreover, a growing number of reports suggest that embryo manipulation *in vitro* increases the risk of diseases caused by aberrant DNA methylation patterns, such as Angelman syndrome (AS) and Beckwith–Wiedemann syndrome (BWS) [30–34]. Nevertheless, the factor(s) that causes DNA methylation instability in *in vitro* manipulated embryos has not yet been identified. Hence, we initiated experiments on the basis of the expectation that Dnmt3bΔ6 is responsible for hypomethylation in *in vitro* manipulated embryos.

Materials and Methods

Animals

C57BL/6J mice (B6, JAX mice), CD1 mice (Charles River, Yokohama, Japan) and F344 rats (CLEA Japan, Tokyo, Japan) were used in this study. All animal experiments were conducted according to the guidelines of the Animal Care and Experimentation Committee of Gunma University, Showa Campus, Japan.

Embryo collection, culture and transfer

C57BL/6J females were superovulated by injection of 5 units of pregnant mare serum (PMSG, ASKA Pharmaceutical, Tokyo, Japan) followed by injection of 5 units of human chorionic gonadotropin 48 h later (hCG, ASKA Pharmaceutical). Females were bred to C57BL/6J males overnight. Approximately 24 h after hCG, the females were sacrificed, and fertilized embryos were collected from the oviducts. These embryos were cultured as IVC blastocysts to the blastocyst stage (114 h after hCG) in M16 medium. In contrast, the *in vivo*-developed blastocysts were collected from uteri 96 h after hCG. The methods used to produce parthenogenetic embryos [35] and SCNT embryos have been described previously [36]. Some of the IVC and *in vivo*-developed blastocysts were transferred to the uterine horns of pseudopregnant recipient females (CD1) 2.5 days postcoitus (dpc), and these embryos were harvested after 7 days (9.5 dpc).

Cell counting of blastocysts

Inner cell mass (ICM) and trophectoderm (TE) cell numbers of blastocysts were counted as previously reported [37].

Generation of ES cell lines

The methods used for generation of ES cell lines have been previously described [35, 38]. Briefly, blastocysts were transferred into gelatinized tissue culture wells (2–3 blastocysts per well of a 4-well multiplate, Nunc, Rochester, NY, USA) and cultured for 7 days in ES medium and DMEM (Gibco, Gland Island, NY, USA) containing 17.5% Knockout SR (Gibco) following standard procedures [39, 40]. After 7 days, ICM outgrowths were harvested in trypsin/EDTA (0.25%/1 mM, Gibco), disaggregated by mouth pipetting and plated onto gelatinized tissue culture wells in ES medium (passage 1). Clones morphologically resembling ES cells were then picked and disaggregated a second time. The cells were then expanded and passaged prior to freezing or use.

DNA isolation and methylation analysis

DNA was isolated from about 10 blastocysts in each pool. Bisulfite treatment was carried out using an EpiTect Bisulfite Kit (Qiagen, Hilden, Germany), according to the manufacturer's instructions. PCR amplification of major and minor satellite DNA was performed for each set of primers:

major satellite,
5'-AAATCTAGAAATGTTTATTGTAGGA-3' and
5'-TTCGGATCCTAAAATATATATTTCTCAT-3';
minor satellite,
5'-TATGGAAAATGATAAAAATTATATTG-3' and
5'-ATTATAACTCATTAATATACACTATTC-3'.

The amplification consisted of a total of 21 cycles at 94 C for 10 sec, 55 C for 30 sec and 72 C for 60 sec for the major satellite primers and a total of 26 cycles at 94 C for 10 sec, 58 C for 30 sec and 72 C for 60 sec for the minor satellite primers using a GeneAmp PCR System 9700 (Applied Biosystems, Foster City, CA, USA). PCR products derived from 3 independent pools were subcloned into a TA cloning vector (pCR 2.1, Invitrogen). Positive clones for each sample were sequenced using the BigDye terminator method (ABI PRISM 3100, Applied Biosystems).

RNA extraction and reverse transcriptase-polymerase chain reaction (RT-PCR)

Total RNA was purified from embryos and nonhuman tissue using TRIzol reagent (Invitrogen, Carlsbad, CA, USA). Total RNA was obtained from human tissue using Human Total RNA Master Panel II (BD Biosciences, San Jose, CA, USA). Purified RNA from 50 blastocysts or 1 μg of purified RNA from postimplantation embryos and tissues was reverse transcribed using Superscript II (TaKaRa, Otsu, Japan) and Oligo(dT)$_{12–18}$ (TaKaRa) in a total volume of 20 μl. The mRNA expression level of each *Dnmt3bs* was determined by PCR using LA Taq HS DNA polymerase (Takara) and the primer sets shown in Table 1. PCR products were separated electrophoretically on a 2.5% agarose gel. For densitometry, the Quantity One software (Bio-Rad, Hercules, CA, USA) was used according to the manufacturer's instructions, and the expression ratios of –exon 6/+exon 6 (–exon 5/+exon 5) were calculated. Quantitative real-time RT-PCR for *Dnmt3b* was also carried out as previously reported [38].

Identification of Dnmt3bΔ6 splice variants

Mouse *Dnmt3b* cDNA was amplified from SCNT ES cells using primers S5 and AS3 (Table 1). PCR products were subcloned into the TA cloning vector (pCR 2.1; Invitrogen). RT-PCR primers for the *Dnmt3b* splice sites (Table 1) were used to identify splice variants. To confirm the variant sequences, the clones were sequenced using the BigDye terminator method (ABI PRISM 3100, Applied Biosystems).

Purification of recombinant Dnmt3b

Recombinant His-tagged Dnmt3b protein was produced in sf9 cells using the baculovirus expression system (Invitrogen) as described previously [41]. The ATG coding initiation methionines

Table 1. Sequences of the primers used for PCR amplification

Gene name		Sequence	Product size	Target
Mouse				
Dnmt3b	S1	gggaacttcagtgaccagtcctc	565 bp	Exon 6
	AS1	ccacctgtgtggtatcca		
	S2	ctggagagtcactggaggaccagctgaagc	290 bp	Exon 11
	AS2	ctctcctcatcctcccctcggtccttc		
	S3	acaaccgtccattcttctgg	391 bp	Catalytic region
	AS3	acgtccgtgtagtgagcaggga		
	S4	ctttcaggaaacaatgaaggga	2716 bp	Full length
	AS4	gctgaggtacagtgatgtga		
	S5	aaagcccggcttctcggaga	2002 bp	Dnmt3bΔ6 variants
	AS3	acgtccgtgtagtgagcaggga		
Gapdh	S	aatgcatcctgcaccaccaa	106 bp	
	AS	gtggcagtgatggcatggac		
Rat				
Dnmt3b	S	gtgaagcggatgatggagat	458 bp	Exon 6
	AS	ctttccccacacaaggtcac		
Gapdh	S	aatgcatcctgcaccaccaa	106 bp	
	AS	gtggcagtgatggcatggac		
Human				
DNMT3B	S	ccaggactcgttcagaaagc	237 bp	Exon 5
	AS	cgtctgtgaggtcgatggta		
GAPDH	S	aatgcctcctgcaccaccaa	106 bp	
	AS	gtggcagtgatggcatggac		

of mouse *Dnmt3b1Δ6* and *Dnmt3b1* were directly ligated using a BamH1 linker without any spacer sequence and then subcloned into the BamH1 site of the multicloning site of the pFAST-BACHTb vector (Invitrogen). Recombinant baculoviruses were constructed according to the manufacturer's instructions, and the viruses were amplified by three rounds of infection to obtain a high-titer baculovirus stock. Sf9 cells were maintained in Grace's medium containing 10% (v/v) fetal bovine serum at 27 C. The recombinant baculoviruses harboring Dnmt3b1Δ6 and Dnmt3b1 were infected into 5×10^8 sf9 cells at an M.O.I. (multiplicity of infection) of 2. After infection, the cells were incubated for 16 or 66 h and then harvested. Purification of His-Dnmt3b was carried out as described previously [41].

DNA methylation activity assay

The DNA methylation activity was determined as described elsewhere [9]. In brief, 50 ng (about 0.5 pmol) of purified Dnmt3b, 0.1 mg of dGdC and 133 pmol (2.0 μCi and 5.3 μM) of [^{3}H]-*S*-adenosyl-L-methionine (AdoMet) (15Ci/mmol, GE Healthcare, Uppsala, Sweden) were added to 25 μl of the reaction buffer (2.7 M glycerol, 5 mM EDTA, 0.2 mM DTT, 40–160 mM NaCl and 20 mM Tris-Hcl at pH 7.4). After a 1-h incubation, the reaction was terminated with 1.5 mM nonradioactive AdoMet. The mixtures were then incubated with 0.1 μg of proteinase K (Nacalai Tesque, Kyoto, Japan) at 50 C for 20 min, and the level of radioactivity was then determined as described previously [42].

Statistical analysis

QUMA (QUantification tool for Methylation Analysis, http://quma.cdb.riken.jp/) was used to statistically analyze the bisulfite sequencing of CpG methylation. The entire set of CpG sites was evaluated with the Mann-Whitney *U*-test. The Student's *t*-test was used for gene expression analysis and cell number analysis. Data are shown as means and standard deviations (SD). A P-value of <0.05 was considered significant.

Results and Discussion

Dnmt3bΔ6 expression in embryos and ES cell lines

A lot of reports have suggested that *in vitro* manipulation causes aberrant DNA methylation patterns (mostly hypomethylation) in the DMRs of imprinted genes in preimplantation embryos, whereas there have been few reports about the methylation patterns in the satellite repeat regions in these embryos. Therefore, we first exam-

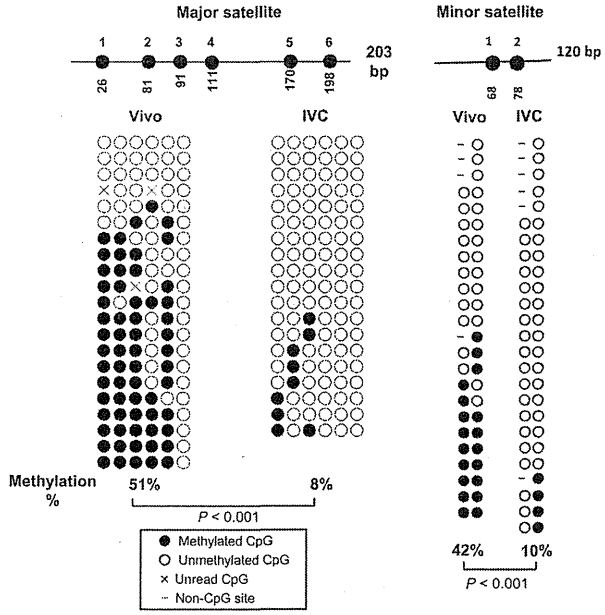

Fig. 1. DNA methylation status of centromeric repeat regions in blastocysts. Hypomethylation of major and minor satellite repeats was observed in *in vitro*-cultured blastocysts (IVC) relative to *in vivo*-developed blastocysts (Vivo).

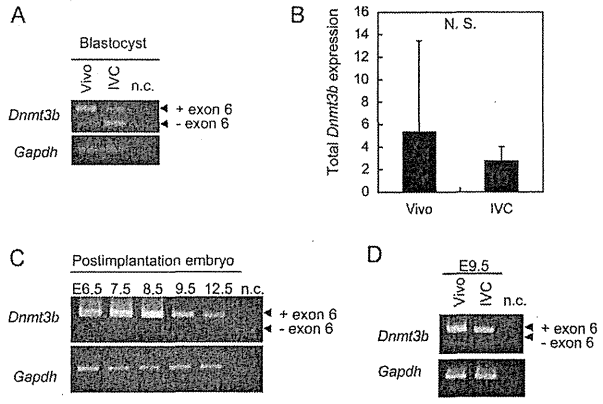

Fig. 2. *Dnmt3bΔ6* (exon 6 splice form) expression in mouse embryos. A: *Dnmt3b* containing exon 6 was the major transcript in blastocysts developed *in vivo* (Vivo), whereas both the spliced and unspliced forms were present in *in vitro*-cultured blastocysts (IVC). n.c., negative control. B: Total *Dnmt3b* expression was not significantly different (N. S.) between Vivo and IVC blastocysts. C: *Dnmt3bΔ6* was detected at very low levels in embryos postimplantation. D: *Dnmt3bΔ6* expression was not detectable in E9.5 fetuses derived from IVC embryos, indicating that the spliced form is expressed in undifferentiated cells and is then repressed during differentiation. n.c., negative control.

Table 2. Means of inner cell mass (ICM), trophectoderm (TE) and total cell number of blastocysts

	Cell number (mean ± SD)			
Blastocysts	Total	ICM	TE	
In vivo (96 h)	43.3 ± 7.4	12.1 ± 2.8	31.2 ± 6.3	(N = 11)
IVC (114 h)	40.0 ± 8.6	12.0 ± 4.4	28.0 ± 6.1	(N = 10)

ined the DNA methylation statuses of these regions, and we found that IVC blastocysts are aberrantly hypomethylated relative to control *in vivo*-derived blastocysts (Fig. 1). Dnmt3b is the primary *de novo* DNA methyltransferase that methylates satellite repeats, especially the centromeric minor satellite repeats [8]. We hypothesized that the abnormal hypomethylation could be caused by the altered expression of specific *Dnmt3b* splicing variants in *in vitro*-manipulated embryos. To determine whether distinct *Dnmt3b* splicing variants were specifically expressed in preimplantation embryos (blastocyst stage), we prepared IVC blastocysts (114 h after hCG) and *in vivo*-developed blastocysts (96 h after hCG). At these times, ICM, TE and total cell numbers were not significantly different between IVC and *in vivo* developed blastocysts, indicating that both embryos were at the same developmental stage (Table 2). RT-PCR using a primer set that recognizes exon 6 splicing variants showed that *Dnmt3bΔ6* was more highly expressed in IVC blastocysts than *in vivo*-developed blastocyst controls (Fig. 2A), although the total Dnmt3b expression levels were not significantly different (Fig. 2B). In general, Dnmt3b is the major *de novo* DNA methyltransferase in E4.5–7.5 embryos, and its expression is down-regulated after midgestation [8, 16]. Our data agree with the findings of these reports (Fig. 2C). In addition, *Dnmt3bΔ6* expression was not detected in *in vivo* embryos during postimplantation development (Fig. 2C). Similarly, *Dnmt3bΔ6* expression was not detectable in E9.5 embryos that were produced by transplantation of IVC blastocysts into pseudopregnant females (Fig. 2D). These results indicate that *Dnmt3bΔ6* is specifically expressed in preimplantation blastocysts. High levels of *Dnmt3bΔ6* were also detected in undifferentiated ES cells generated from *in vitro* manipulated embryos, such as those generated by IVC (Fig. 3A), by parthenogenetic methods or from SCNT blastocysts (Fig. 3B). Thus, *Dnmt3bΔ6* is specifically expressed in undifferentiated cell types such as preimplantation embryos manipulated *in vitro* and their derivative ES cells.

Identification of Dnmt3bΔ6 splice variants

At least 16 *Dnmt3b* variants have been described in mice [22]; therefore, we performed PCR analysis using a primer set that amplified exon 6-deleted forms, and the PCR products were subcloned into a TA cloning vector. Each clone was characterized by

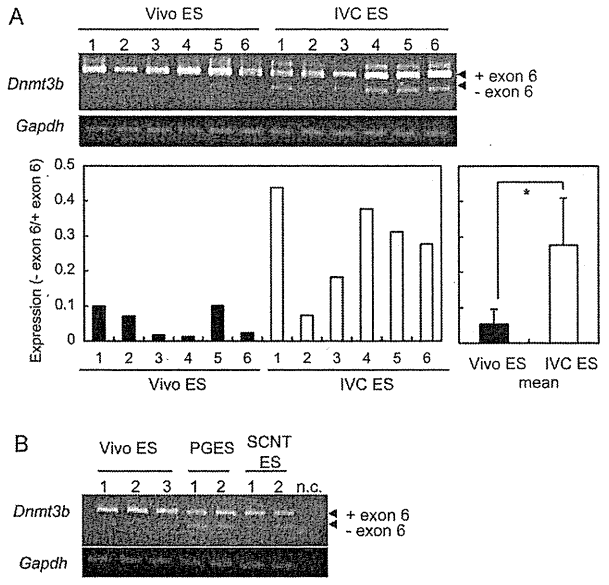

Fig. 3. *Dnmt3bΔ6* (exon 6 splice form) expression in mouse ES cells. A: *Dnmt3bΔ6* was more highly expressed in IVC embryo-derived ES cells (IVC ES) than in ES cells generated from *in vivo*-developed blastocysts (Vivo ES). * P<0.05. B: *Dnmt3bΔ6* was more highly expressed in ES cells that had been generated from *in vitro*-manipulated embryos, such as those generated by parthenogenesis (PG) and somatic cell nuclear transfer (SCNT). n.c., negative control.

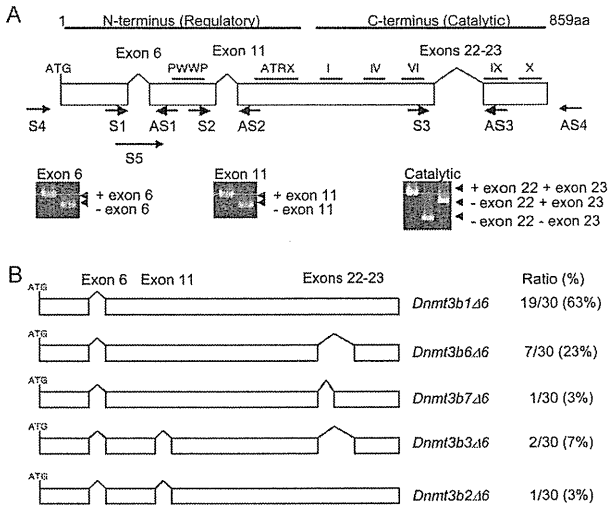

Fig. 4. Identification of mouse *Dnmt3bΔ6* splice variants. A: *Upper panel*: map of *Dnmt3b* mRNA showing the positions of conserved domains. *Arrows*: locations of the RT-PCR primers used in this study. *Lower panel*: RT-PCR analysis of cloned alternative splicing variants identified those lacking exons 6, 11 and 22–23. B: Organization of the *Dnmt3bΔ6* mRNA species present in SCNT ES cells. The PCR products amplified from *Dnmt3bΔ6* cDNA were subcloned into a TA cloning vector, and each clone was characterized by sequencing. The most common form of *Dnmt3b1Δ6* identified was *Dnmt3b1Δ6* (63%), while the second most common form was *Dnmt3b6Δ6* (23%).

RT-PCR and sequencing to identify individual variants. From these analyses, five variants lacking exon 6 were identified. The most prevalent form identified was *Dnmt3b1Δ6* (63%), which only lacked exon 6, and the second most common form was *Dnmt3b6Δ6* (23%), which lacked exon 6 and exons 22–23 of the catalytic domain (Fig. 4A and B).

DNA methylation activity of purified Dnmt3bΔ6

To determine the DNA methylation activity of Dnmt3b1Δ6 *in vitro*, sf9 cells were infected with recombinant baculoviruses encoding Dnmt3b1 and Dnmt3b1Δ6, and recombinant Dnmt3b1 and Dnmt3b1Δ6 were then purified (Fig. 5A and B). Dnmt3b1Δ6 demonstrated DNA methylation activity, although it showed lower activity than the control Dnmt3b1 (Fig. 5C). The second major variant, Dnmt3b6Δ6, which lacks the catalytic domain, was not examined; however, Dnmt3b6Δ6 is not expected to possess methylation activity, as all the other mouse Dnmt3b variants without the catalytic domain (e.g., Dnmt3b3) do not possess methylation activity. Thus, we concluded that there would be insufficient methylation activity in cells, such as IVC blastocysts, in which the dominant Dnmt3b form is Dnmt3bΔ6.

Tissue- and species-specific expression of Dnmt3bΔ6

According to the NCBI (National Center for Biotechnology Information) database, the exon 6 region is highly conserved among mice, rats and humans. To determine the expression pattern of *Dnmt3bΔ6* in these species, RT-PCR was performed using exon 6-specific primer sets. In mice, only low levels of *Dnmt3bΔ6* expression were observed in all tissues except for skeletal muscle (Fig. 6A). A very low level of *Dnmt3bΔ6* expression was also seen in rat tissues (Fig. 6B). Human *DNMT3B* lacks one noncoding exon at its 5'-end; therefore, the region equivalent to exon 6 in mouse *Dnmt3b* is exon 5 in human *DNMT3B*. Interestingly, the highest levels of human *DNMT3B* lacking exon 5 (*DNMT3BΔ5*) expression were observed in both the adult and fetal brain (Fig. 6 C). DNMT3B is reported to be necessary for nerve growth factor-mediated differentiation [43], and the DNMT3B mutations that occur in ICF syndrome lead to altered epigenetic modifications and aberrant expression of genes regulating neurogenesis [44]. This variant is thus proposed to be necessary for the development and maintenance of neural function in humans. In contrast, only a low level of *Dnmt3bΔ6* expression was observed in mouse and rat brains. The reason for the difference between human and rodent *Dnmt3b* expression is presently unclear. Further studies will be required to elucidate the specific roles of Dnmt3bΔ6 in neural development.

Dnmt3bΔ6 and centromeric hypomethylation

In vitro manipulated embryos often exhibit abnormal methylation patterns in genomic imprinting regions and centromeric repeats. In this study, we have shown the first evidence that *Dnmt3bΔ6*, which is highly expressed in *in vitro* manipulated

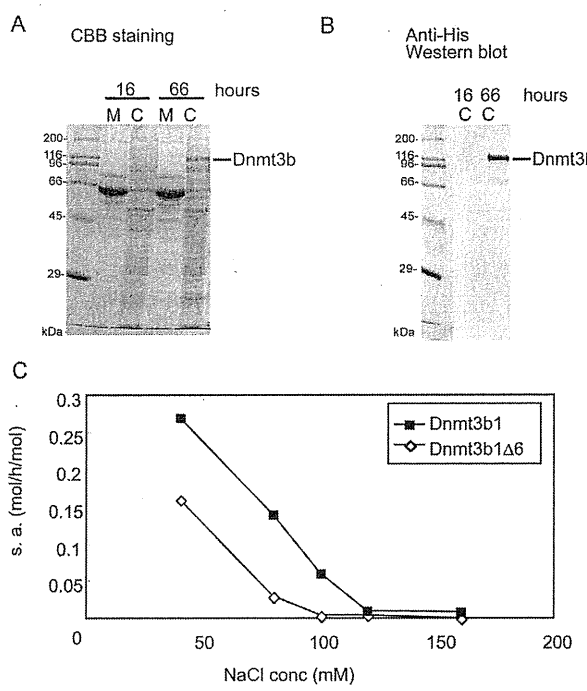

Fig. 5. *De novo* methylation activity of purified Dnmt3bΔ6. A: Recombinant baculoviruses encoding Dnmt3bΔ6 were generated and used to infect sf9 cells. Samples obtained 16 and 66 h after infection were subjected to SDS-PAGE and then stained with CBB. M, medium fraction; C, cell fraction. B: Purified protein was blotted with an anti-His antibody. C: The DNA methylation activity [specific activity (s.a.) in mol/h/mol] of Dnmt3b1Δ6 and Dnmt3b1 was titrated with NaCl.

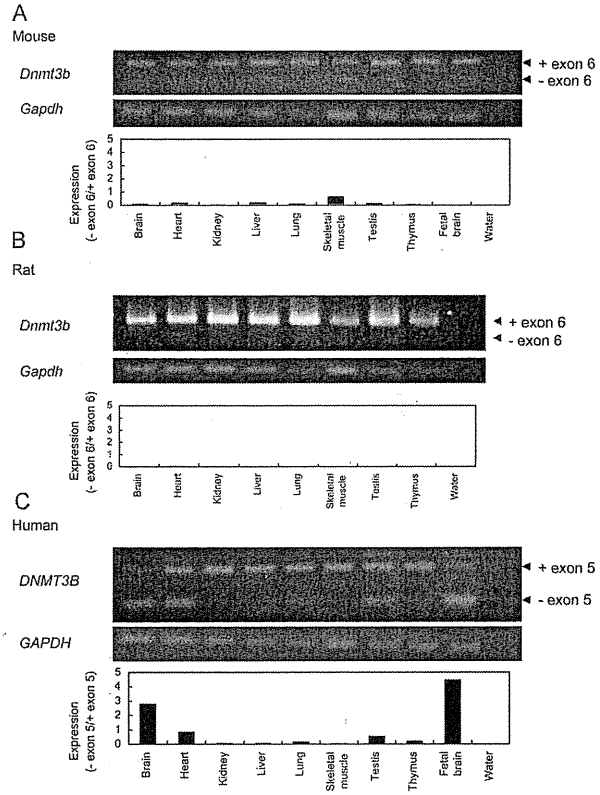

Fig. 6. *Dnmt3bΔ6* (*DNMT3BΔ5*) expression in various tissues. *Dnmt3b* containing exon 6 was the abundantly expressed variant in mouse tissues (A) and in rat tissues (B). C: In humans, *DNMT3B* lacking exon 5 was the predominant form in adult and fetal brains.

embryos, may be involved in abnormal DNA methylation. *Dnmt3bΔ6* (*DNMT3BΔ5*) is also overexpressed in human cancer cell lines [24] that often exhibit global hypomethylation, where it primarily affects repetitive regions of the genome, such as the centromeric and pericentromeric regions [45]. Notably, ectopic overexpression of DNMT3B3Δ5 resulted in repetitive element hypomethylation in cancer cells [24]. Thus, Dnmt3bΔ6 could be involved in DNA hypomethylation, especially in the centromeric and pericentromeric satellite repeat region in early embryos. After fertilization, the embryonic genome, including the centromeric satellite repeats, becomes demethylated, and these methylation levels are maintained during preimplantation development [46, 47]. Even blastocysts that develop *in vivo* exhibit low levels of *Dnmt3bΔ6* expression, implying that Dnmt3bΔ6 is essential for demethylation or maintenance of the methylation status of centromeric satellite repeats. Consistent with this hypothesis, excessive expression of *Dnmt3bΔ6* in IVC embryos may induce abnormal DNA methylation. Thus, the expression pattern of Dnmt3bΔ6 and other Dnmt3b variants seems to be precisely regulated at the preimplantation stage. Although we do not have information about how *Dnmt3b* splicing is regulated, small nuclear ribonucleoprotein particles (snRNPs) and their mediator SF2/ASF [48, 49] are likely candidates.

In vitro embryo manipulation technologies have contributed to the development of infertility treatments and new animal reproduction strategies. However, *in vitro* embryo manipulation increases the risk of epigenetic abnormalities, a crucial problem that remains to be solved. Our findings regarding Dnmt3bΔ6 expression may provide clues as to why epigenetic abnormalities occur in embryos manipulated *in vitro*.

Acknowledgments

We thank Dr S Ikeda (Kyoto University) for his technical advice regarding sf9 cell culture and cell counting of blastocysts. This study was supported in part by grants from the Japanese Science and Technology Agency; the National Institute of Biomedical Innovation; the Ministry of Education, Culture, Sports, Science and Technology of Japan; the Takeda Science Foundation; joint research program of the Institute for Molecular and Cellular Regulation, Gunma University; and the Ministry of Health, Labour, and Welfare of Japan.

References

1. **Antequera F, Bird A.** CpG islands in DNA methylation. *In*: Jost JP, Saluz HP (eds.), Molecular Biology and Biological Significance. Basel: Birkhauser Verlag; 1993: 169–185.
2. **Jaenisch R.** DNA methylation and imprinting: why bother? *Trends Genet* 1997; 13: 323–329.
3. **Jones P, Gonzalgo M.** Altered DNA methylation and genome instability: a new pathway to cancer? *Proc Natl Acad Sci USA* 1997; 94: 2103–2105.
4. **Robertson KD, Wolffe AP.** DNA methylation in health and disease. *Nat Rev Genet* 2000; 1: 11–19.
5. **Surani MA.** Imprinting and the initiation of gene silencing in the germline. *Cell* 1998; 93: 309–312.
6. **Monk M.** Changes in DNA methylation during mouse embryonic development in relation to X-chromosome activity and imprinting. *Phil Trans R Soc Lond* 1990; 326: 299–312.
7. **Okano M, Xie S, Li E.** Cloning and characterization of a family of novel mammalian DNA (cytosine-5) methyltransferases. *Nat Genet* 1998; 19: 219–220.
8. **Okano M, Bell DW, Haber DA, Li E.** DNA methyltransferases Dnmt3a and Dnmt3b are essential for *de novo* methylation and mammalian development. *Cell* 1999; 99: 247–257.
9. **Aoki A, Suetake I, Miyagawa J, Fujio T, Chijiwa T, Sasaki H, Tajima S.** Enzymatic properties of *de novo*-type mouse DNA (cytosine-5) methyltransferases. *Nucleic Acids Res* 2001; 29: 3506–3512.
10. **Gowher H, Jeltsch A.** Enzymatic properties of recombinant Dnmt3a DNA methyltransferase from mouse: The enzyme modifies DNA in a non-processive manner and also methylates non-CpG sites. *J Mol Biol* 2001; 309: 1201–1208.
11. **Lin IG, Han L, Taghva A, O'Brien LE, Hsieh CL.** Murine de novo methyltransferase Dnmt3a demonstrates strand asymmetry and site preference in the methylation of DNA *in vitro*. *Mol Cell Biol* 2002; 22: 704–723.
12. **Yokochi T, Robertson KD.** Preferential methylation of unmethylated DNA by mammalian *de novo* DNA methyltranasferase Dnmt3a. *J Biol Chem* 2002; 277: 11735–11745.
13. **Liang G, Chan M, Tomigahara Y, Tsai YC, Gonzales FA, Li E, Laird PW, Jones PA.** Cooperativity between DNA methyltransferases in the maintenance methylation of repetitive elements. *Mol Cell Biol* 2002; 22: 480–491.
14. **Rhee I, Bachman KE, Park BH, Jair KW, Yen RW, Schuebel KE, Cui H, Feinberg AP, Lengauer C, Kinzler KW, Baylin SB, Vogelstein B.** DNMT1 and DNMT3b cooperate to silence genes in human cancer cells. *Nature* 2002; 416: 552–556.
15. **Kim GD, Ni J, Kelesoglu N, Roberts RJ, Pradhan S.** Co-operation and communication between the human maintenance and *de novo* DNA (cytosine-5) methyltransferases. *EMBO J* 2002; 21: 4183–4195.
16. **Watanabe D, Suetake I, Tada T, Tajima S.** Stage- and cell-specific expression of Dnmt3a and Dnmt3b during embryogenesis. *Mech Dev* 2002; 118: 187–190.
17. **Hansen RS, Wijmenga C, Luo P, Stanek AM, Canfield TK, Weemaes CM, Gartler SM.** The DNMT3B DNA methyltransferase gene is mutated in ICF immunodeficiency syndrome. *Proc Natl Acad Sci USA* 1999; 96: 14412–14417.
18. **Xu GL, Bestor TH, Bourc'his D, Hsieh C, Tommerup N, Bugge M, Hulten M, Qu X, Russo JJ, Viegas-Pequignot E.** Chromosome instability and immunodeficiency syndrome caused by mutations in a DNA methyltransferase gene. *Nature* 1999; 402: 187–190.
19. **Robertson KD, Uzvolgy E, Liang G, Talmadge C, Sumegi J, Gonzales FA, Jones PA.** The human DNA methyltransferases (DNMTs) 1, 3a and 3b: coordinate mRNA expression in normal tissues and overexpression in tumors. *Nucleic Acids Res* 1999; 27: 2291–2298.
20. **Xie S, Wang Z, Okano M, Nogami M, Li Y, He WW, Okumura K, Li E.** Cloning, expression and chromosome locations of the human DNMT3 gene family. *Gene* 1999; 236: 87–95.
21. **Chen T, Ueda Y, Xie S, Li E.** A novel Dnmt3a isoform produced from an alternative promoter localizes to euchromatin and its expression correlates with active *de novo* methylation. *J Biol Chem* 2002; 277: 38746–38754.
22. **Weisenberger DJ, Velicescu M, Cheng JC, Gonzales FA, Liang G, Jones PA.** Role of the DNA methyltransferase variant DNMT3b3 in DNA methylation. *Mol Cancer Res* 2004; 2: 62–72.
23. **Chen T, Ueda Y, Dodge JE, Wang Z, Li E.** Establishment and maintenance of genomic methylation patterns in mouse embryonic stem cells by Dnmt3a and Dnmt3b. *Mol Cell Biol* 2003; 23: 5594–5605.
24. **Gopalakrishnan S, Van Emburgh BO, Shan J, Su Z, Fields CR, Vieweg J, Hamazaki T, Schwartz PH, Terada N, Robertson KD.** A novel DNMT3B splice variant expressed in tumor and pluripotent cells modulates genomic DNA methylation patterns and displays altered DNA binding. *Mol Cancer Res* 2009; 7: 1622–1634.
25. **Saito Y, Kanai Y, Sakamoto M, Saito H, Ishii H, Hirohashi S.** Overexpression of a splice variant of DNA methyltransferase 3b, DNMT3b4, associated with DNA hypomethylation on pericentromeric satellite regions during human hepatocarcinogenesis. *Proc Natl Acad Sci USA* 2002; 99: 10060–10065.
26. **Doherty AS, Mann MR, Tremblay KD, Bartolomei MS, Schultz RM.** Differential effects of culture on imprinted *H19* expression in the preimplantation mouse embryo. *Biol Reprod* 2000; 62: 1526–1535.
27. **Khosla S, DeanW, Brown D, ReikW, Feil R.** Culture of preimplantation mouse embryos affects fetal development and the expression of imprinted gene. *Biol Reprod* 2001; 64: 918–926.
28. **Li T, Vu TH, Ulaner GA, Littman E, Ling JQ, Chen HL, Hu JF, Behr B, Giudice L, Hoffman AR.** IVF results in *de novo* DNA methylation and histone methylation at an *Igf2-H19* imprinting epigenetic switch. *Mol Hum Reprod* 2005; 11: 631–640.
29. **Zaitseva I, Zaitsev S, Alenina N, Bader M, Krivokharchenko A.** Dynamics of DNA-demethylation in early mouse and rat embryos developed *in vivo* and *in vitro*. *Mol Reprod Dev* 2007; 74: 1255–1261.
30. **Cox GF, Burger J, Lip V, Mau UA, Sperling K, Wu BL, Horsthemke B.** Intracytoplasmic sperm injection may increase the risk of imprinting defects. *Am J Hum Genet* 2002; 71: 162–164.
31. **DeBaun MR, Niemitz EL, Feinberg AP.** Association of *in vitro* fertilization with Beckwith-Wiedemann syndrome and epigenetic alterations of LIT1 and H19. *Am J Hum Genet* 2003; 72: 156–160.
32. **Gicquel C, Gaston V, Mandelbaum J, Siffroi JP, Flahault A, Le Bouc Y.** *In vitro* fertilization may increase the risk of Beckwith-Wiedemann syndrome related to the abnormal imprinting of the KCN1OT gene. *Am J Hum Genet* 2003; 72: 1338–1341.
33. **Maher ER, Brueton LA, Bowdin SC, Luharia A, Cooper W, Cole TR, Macdonald F, Sampson JR, Barratt C, Reik W, Hawkins MM.** Beckwith-Wiedemann syndrome and assisted reproduction technology (ART). *J Med Genet* 2003; 40: 62–64.
34. **Orstavik KH, Eiklid K, van der Hagen CB, Spetalen S, Kierulf K, Skjeldal O, Buiting K.** Another case of imprinting defect in a girl with Angelman syndrome who was conceived by intracytoplasmic semen injection. *Am J Hum Genet* 2003; 72: 218–219.
35. **Horii T, Kimura M, Morita S, Nagao Y, Hatada I.** Loss of genomic imprinting in mouse parthenogenetic embryonic stem cells. *Stem Cells* 2008; 26: 79–88.
36. **Ogura A, Inoue K, Takano K, Wakayama T, Yanagimachi R.** Birth of mice after nuclear transfer by electrofusion using tail tip cells. *Mol Reprod Dev* 2000; 57: 55–59.
37. **Thouas GA, Korfiatis NA, French AJ, Jones GM, Trounson AO.** Simplified technique for differential staining of inner cell mass and trophectoderm cells of mouse and bovine blastocysts. *Reprod Biomed Online* 2001; 3: 25–29.
38. **Horii T, Yanagisawa E, Kimura M, Morita S, Hatada I.** Epigenetic differences between embryonic stem cells generated from blastocysts developed *in vitro* and *in vivo*. *Cell Reprogram* 2010; 12: 551–563.
39. **Robertson EJ.** Embryo derived stem cell lines. *In*: Robertson EJ (ed.), Teratocarcinomas and Embryonic Stem Cells: A Practical Approach. Oxford: IRL Press; 1987: 71–112.
40. **Horii T, Nagao Y, Tokunaga T, Imai H.** Serum-free culture of murine primordial germ cells and embryonic germ cells. *Theriogenology* 2003; 59: 1257–1264.
41. **Suetake I, Miyazaki J, Murakami C, Takeshima H, Tajima S.** Distinct enzymatic properties of recombinant mouse DNA methyltransferases Dnmt3a and Dnmt3b. *J Biochem* 2003; 133: 737–744.
42. **Kimura H, Suetake I, Tajima S.** Xenopus maintenance-type DNA methyltransferase is accumulated in and translocated into germinal vesicles of oocytes. *J Biochem* 1999; 125: 1175–1182.
43. **Bai S, Ghoshal K, Datta J, Majumder S, Yoon SO, Jacob ST.** DNA methyltransferase 3b regulates nerve growth factor-induced differentiation of PC12 cells by recruiting histone deacetylase 2. *Mol Cell Biol* 2005; 25: 751–766.
44. **Jin B, Tao Q, Peng J, Soo HM, Wu W, Ying J, Fields CR, Delmas AL, Liu X, Qiu J, Robertson KD.** DNA methyltransferase 3B (DNMT3B) mutations in ICF syndrome lead to altered epigenetic modifications and aberrant expression of genes regulating development, neurogenesis and immune function. *Hum Mol Genet* 2008; 17: 690–709.
45. **Jones PA, Baylin SB.** The fundamental role of epigenetic events in cancer. *Nature Rev Genet* 2002; 3: 415–428.
46. **Kim SH, Kang YK, Koo DB, Kang MJ, Moon SJ, Lee KK, Han YM.** Differential DNA methylation reprogramming of various repetitive sequences in mouse preimplantation embryos. *Biochem Biophys Res Commun* 2004; 324: 58–63.
47. **Fernandez-Gonzalez R, Ramirez MA, Bilbao A, De Fonseca FR, Gutierrez-Adan A.** Suboptimal *in vitro* culture conditions: an epigenetic origin of long-term health effects. *Mol Reprod Dev* 2007; 74: 1149–1156.
48. **Krainer AR, Conway GC, Kozak D.** Purification and characterization of pre-mRNA splicing factor SF2 from HeLa cells. *Genes Dev* 1990 ; 4: 1158–1171.
49. **Krainer AR, Conway GC, Kozak D.** The essential pre-mRNA splicing factor SF2 influences 5' splice site selection by activating proximal sites. *Cell* 1990; 62: 35–42.

Generation of genetically modified rats from embryonic stem cells

Masaki Kawamata and Takahiro Ochiya[1]

Section for Studies on Metastasis, National Cancer Center Research Institute, 1-1 Tsukiji, 5-chome, Chuo-ku, Tokyo 104-0045, Japan

Communicated by Takashi Sugimura, National Cancer Center, Tokyo, Japan, June 30, 2010 (received for review April 22, 2010)

At present, genetically modified rats have not been generated from ES cells because stable ES cells and a suitable injection method are not available. To monitor the pluripotency of rat ES cells, we generated *Oct4*-Venus transgenic (Tg) rats via a conventional method, in which Venus is expressed by the *Oct4* promoter/enhancer. This monitoring system enabled us to define a significant condition of culture to establish authentic rat ES cells based on a combination of 20% FBS and cell signaling inhibitors for Rho-associated kinase, mitogen-activated protein kinase, TGF-β, and glycogen synthase kinase-3. The rat ES cells expressed ES cell markers such as *Oct4*, *Nanog*, *Sox2*, and *Rex1* and retained a normal karyotype. Embryoid bodies and teratomas were also produced from the rat ES cells. All six ES cell lines derived from three different rat strains successfully achieved germline transmission, which strongly depended on the presence of the inhibitors during the injection process. Most importantly, high-quality Tg rats possessing a correct transgene expression pattern were successfully generated via the selection of gene-manipulated ES cell clones through germline transmission. Our rat ES cells should be sufficiently able to receive gene targeting as well as Tg manipulation, thus providing valuable animal models for the study of human diseases.

genetic engineering | rat | embryonic stem cells

The laboratory rat was the earliest mammalian species domesticated for scientific research and has been used as an animal model in physiology, toxicology, nutrition, behavior, immunology, and neoplasia for over 150 y (1). Despite this history, rats lag far behind mice in functional genetic studies and the generation of knockout animal models reflecting human diseases because of the absence of germline-competent rat ES cells, which are vital in a reverse genetics approach (2, 3). Recently, gene-targeting rats were created by the zinc finger nuclease strategy (4). However, the system is not available for most researchers because a special technique is required to make algorithm-based sequence-specific DNA nucleases. Thus, establishment of rat ES cells has been desired to produce gene-targeting rats, such as mutant mice, routinely.

Although we established rat ES cell lines with chimeric contribution, none could complete germline transmission (5). Soon after our report, other groups succeeded in establishing rat ES cells with germline transmission by using 2i, mitogen-activated protein kinase (MEK) inhibitor PD0325901, and glycogen synthase kinase-3 (GSK3) inhibitor CHIR99021 (6, 7). The 2i is widely used in the establishment of ES cells or induced pluripotent stem (iPS) cells in mice (8, 9), rats (6, 7, 10), and humans (10). Thus, the inhibition of MEK and GSK3 has been thought to maintain a ground state of pluripotency in various species. Rat iPS cells with chimeric contribution were established by using an inhibitor of type 1 TGF-β receptor Alk5 (A-83-01) with the 2i, although germline transmission was not accomplished (10). Furthermore, a combination of MEK and ALK5 inhibitors dramatically improved the efficiency of iPS cell generation from human fibroblasts (11). These reports indicate that the inhibition of TGF-β signaling also plays a key role in pluripotency.

It is known that rat ES cells present critical problems in that undifferentiated cells cannot proliferate from single cells after enzymatic dissociation (5) and that chromosomal instability is caused by long-term culture, resulting in the failure of germline transmission (5–7). Recently, Watanabe et al. found that a Rho-associated kinase inhibitor Y-27632 (12) blocks apoptosis and enhances the proliferation of human ES cells after their dissociation into single cells by enzymatic treatment (13). The propagated ES cells cultured by Y-27632 were positive for alkaline phosphatase (ALP) and marker genes such as E-cadherin, Oct4, and SSEA4, and the number of chromosomes was normally maintained during long-term culture (13). These recent reports indicate the suitability of cell signaling inhibitors in the establishment of rat ES cells.

To generate genetically modified rats, highly potent ES cells that can stably contribute to germline chimeras have to be established. As a first step, we generated *Oct4*-Venus transgenic (Tg) rats, in which Venus [YFP mutant (14)] is expressed by the *Oct4* promoter/enhancer. This Tg line enables us to monitor the pluripotency of rat ES cells during the process of establishment. We addressed suitable combinations of the signaling inhibitors based on a culture medium that included 20% FBS. As a result, the use of a combination of four inhibitors, Y-27632, PD0325901, A-83-01, and CHIR99021 (termed YPAC), allowed the establishment of authentic rat ES cells and appeared necessary in the blastocyst injection process for the generation of germline chimeras. Finally, we report that high-quality Tg rats retaining reproductive ability can be generated from rat ES cells.

Results

YPAC Maintains Pluripotency in the Outgrowths of *Oct4*-Venus Tg Blastocysts. We first generated a Tg rat carrying an *Oct4*-Venus fluorescence reporter to monitor pluripotency during establishment of rat ES cells and to investigate development of the ES cells into germ cells in fetal gonads of chimeras. The 3.9-kb *Oct4* (also known as *Pou5f1*) promoter includes both the proximal enhancer and distal enhancer, which gives *Oct4* expression in morula, inner cell mass (ICM), epiblast, primordial germ cells (PGCs), and ES cells (15). In the Tg embryo, Venus was detected specifically in PGCs in the gonad (Fig. S1). This result corresponds to previous reports regarding *Oct4*-reporter Tg mice (16).

Outgrowths were examined from the Tg blastocysts in a basic medium containing 20% FBS, which is generally used for mouse ES cell culture, with or without YPAC. In its absence, Venus fluorescence was decreased at day 3 after plating and disappeared at day 7 despite the fact that ES-like cells propagated and formed a domed structure similar to the mouse ES cell colony (Fig. 1*A*). In the presence of YPAC, ICM cells rapidly propagated while maintaining Venus fluorescence even at day 7. The fluorescence was not observed in differentiated cells (Fig. 1*B*). The expression levels of ES cell marker genes *Oct4*, *Nanog*, *Sox2*, and *Rex1* in ICM cells with YPAC were higher than those without YPAC (Fig. 1*C*).

Author contributions: M.K. and T.O. designed research; M.K. performed research; M.K. analyzed data; and M.K. and T.O. wrote the paper.

The authors declare no conflict of interest.

Freely available online through the PNAS open access option.

[1]To whom correspondence should be addressed. E-mail: tochiya@ncc.go.jp.

This article contains supporting information online at www.pnas.org/lookup/suppl/doi:10.1073/pnas.1009582107/-/DCSupplemental.

DEVELOPMENTAL

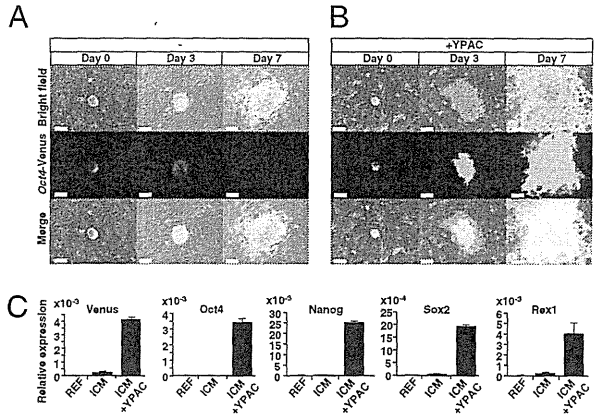

Fig. 1. Outgrowth of ICM cells in YPAC medium. Outgrowth of blastocysts in –YPAC (*A*) or +YPAC (*B*) medium. E4.5 blastocysts were plated onto mitotically inactivated MEFs. (*C*) qPCR analysis of Venus, *Oct4*, *Nanog*, *Sox2*, and *Rex1* in ICM cells. Seven days after plating, RNAs were extracted from domed segments of ICM cells derived from seven or four blastocysts in –YPAC or +YPAC medium, respectively. Transcript levels were normalized to *Gapdh* levels. Data are the mean ± SD of one biological sample assayed in three independent experiments and represent relative expression levels of indicated genes in REFs, ICM (–YPAC), and ICM (+YPAC). (Scale bars: 100 μm.)

In its absence, the decrease of *Oct4* mRNA was parallel to that of Venus mRNA and fluorescence. In the YPAC condition, blastocyst outgrowth was observed in 51 samples for all the tested embryos regardless of the strains (Table 1). The blastocyst strains were derived from a hybrid of Tg Wistar and wild-type Wistar (TgWW, albino), wild-type Wistar (WW, albino), Long–Evans agouti [LEA (LL, agouti)], or a hybrid of Tg Wistar and LEA (TgWL, agouti).

Small Molecules Enable Efficient Derivation and Maintenance of Rat ES Cells. The outgrowths were dissociated into small pieces and replated in the same mouse embryonic fibroblasts (MEFs)/YPAC condition. After undifferentiated colonies appeared, they were split into single cells by Accutase (Innovative Cell Technologies, Inc.). These cells attached on the MEFs and formed domed colonies, which can be passaged continuously (Fig. 2*A Upper Left*). Although most of the ES cells showed ALP activity (Fig. 2*B Left*) and Oct4 protein expression (Fig. 2*D Left*) even after long passages, Venus fluorescence became weak or negative (Fig. 2*A Lower Left*). The expression pattern of Venus mRNA was not parallel to that of *Oct4* between TgWL1 and TgWW1 cell lines (Fig. 2*C*). These results suggest that the function of the *Oct4*-Venus transgene is unavailable in rat ES cell lines. The long-passaged rat ES cells might receive epigenetic silencing effects.

The ES cell lines maintained higher mRNA levels of ES cell marker genes *Oct4*, *Sox2*, *Nanog*, and *Rex1* compared with rat embryonic fibroblasts (REFs) (Fig. 2*C*). Microarray analyses also indicated that global gene expression was remarkably different between ES cells and REFs but similar between the three ES cell lines TgWL1, TgWW1, and LL1 (Fig. S2). Nanog and Sox2 proteins were also detected in ES cells (Fig. 2*D*). The karyotypes of 50 cells were analyzed by G-band staining. Most of the cells exhibited a normal chromosomal number of 42 in TgWL1 (70%, XX, P14), TgWL2 (84%, XX, P7; Fig. 2*E*), TgWW1 (92%, XX, P5), and LL1 (84%, XX, P6). TgWW1 cells (2.6×10^6) could form a teratoma 34 d after transplantation under the skin of an immunodeficient SCID mouse. A histological examination showed that the tumor contained all three germ layers, including the intestinal epithelium (endoderm), cartilage (mesoderm), and neuronal rosette (ectoderm) (Fig. 2*F*).

Table 1. Establishment of rat ES cells from blastocysts in YPAC medium

Strain	No. ICMs	Outgrowth†	Continue	Cell line‡
TgWL	2	2	2	2
TgWW	15	15	1	1
WW	9	9	1	1
LL	19	19	2	2
TgWW*	3	3	2	2
WW*	3	3	0	0
Total	51	51 (100%)	8	8 (100%)

*Specific serum was used (FBS for MEF culture; EQUITECH-BIO, Inc.).
†Outgrowth refers to the expansion of the ICM.
‡Cell line refers to continuous culture of at least seven passages. Single-cell passage was begun at passages 1–3. Domed colonies with undifferentiated cells are continuously formed from single cells.

To confirm the effect of Y, the rat ES cells were cultured in a PAC medium. Under this condition, sparse colonies appeared because of a failure in the adherence process of single cells on MEFs, although the colonies kept undifferentiated morphology and ALP activity (Fig. 2*A Middle* and *B Middle*). Although only Y enabled most of the single cells to adhere on MEFs and to proliferate, they were differentiated and did not show ALP activity (Fig. 2*A Right* and *B Right*).

The classic method to induce ES cell differentiation is to allow the cells to grow in suspension and to form 3D aggregates known as embryoid bodies (EBs) (17). Dissociated ES cells were plated into low-cell-binding dishes in the basal medium. EBs could be formed from the ES cells at a much lower efficiency compared with their formation from mouse ES cells (Fig. 2*E*). The expression of marker genes was decreased during the process of EB differentiation (Fig. 2*I*). In the presence of PAC, cells aggregated with high efficiency and formed a clear 3D structure (Fig. 2*F*). The EBs with PAC at day 7 still sustained high expression levels of the marker genes (Fig. 2*I*). These results suggest that PAC enables ES cells to maintain pluripotency, whereas for rat ES cells to adhere on MEFs, Y is necessary.

YPAC Injection Engenders Germline Chimeras. First, we produced stable transfectant ES cells expressing cyan fluorescence from a CAG-AmCyan1 transgene to monitor cell fate in the blastocyst after injection or chimerism in fetuses (Fig. 3*A*). Before generation of the chimera, the potential of YPAC was investigated during the injection and blastocyst incubation processes because the rat ES cells tended to differentiate easily in the absence of inhibitors (Fig. 2 *A*, *B*, and *E*). There was no difference between normal and YPAC injection 5 h after incubation; in both cases, several cyan-positive cells adhered on the ICM and trophectoderm. However, 30 h after incubation, few cyan-positive cells existed in the blastocysts in the absence of YPAC, whereas in its presence, several cells remained on the ICM surface. Furthermore, blastocyst shape was maintained by the addition of YPAC even after incubation for 30 h (Fig. 3*B*). This result suggests that administration of YPAC during the injection process causes both ES cells and recipient blastocysts to block differentiation or apoptosis. This YPAC injection method enabled generation of chimeric embryos showing positivity for cyan but negativity for Venus in the surface of skin and kidney. Venus-positive cells were detected specifically in the gonads, showing the successful development of the ES cells into germ cells (Fig. 3*C*). We also succeeded in generating germline chimeras using all other cell lines by detecting Venus fluorescence in the fetal gonad (Table 2). The germline chimeras were detected in 2 of 12 fetuses by using long-cultured TgWL2 cells at passage 22 (Table 2 and Fig. S3).

To investigate the pluripotent ability of ES cells, we carried out a single-cell injection into a blastocyst. After injection of the

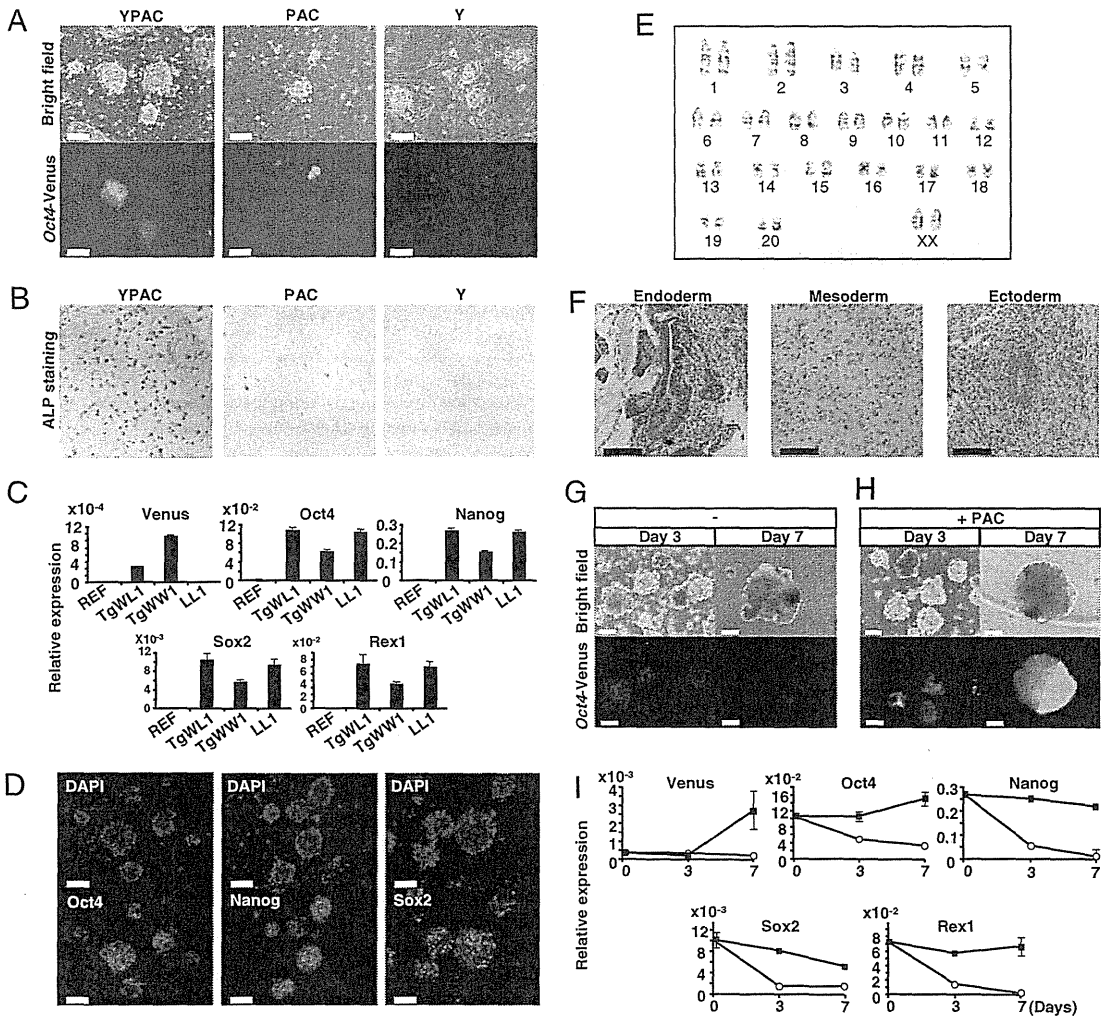

Fig. 2. Characterization of rat ES cells. Effect of Y-27632 (*A*) and ALP (*B*) staining. Dissociated single cells (1×10^5 TgWW1, passage 6) were plated into a well of six-well plates under the condition of MEFs with YPAC (*Left*), PCA (*Center*), or Y (*Right*). (*B*) ALP staining in these cells. (*C*) qPCR analysis of Venus, *Oct4*, *Nanog*, *Sox2*, and *Rex1* in rat ES cell lines. Transcript levels were normalized to *Gapdh* levels. Data are the mean ± SD of one biological sample assayed in three independent experiments and represent the relative expression levels of indicated genes in REF, TgWL1, TgWW1, and LL1. (*D*) Immunofluorescence staining for *Oct4*, *Nanog*, and *Sox2* in rat ES cells. (*E*) Cytogenetic analysis in rat ES cells by G-band staining. Representative data of TgWL2 at passage 7 indicate a chromosomal number of 42, including an XX gender chromosome. (*F*) Histological sections of a teratoma derived from a TgWW1 ES cell line showing three germ layers. Embryoid bodies (TgWL1) were produced in a basic ES cell medium with (*H*) or without (*G*) three PAC inhibitors, excluding Y-27632. A time-course experiment was performed, and the EBs were observed at days 3 and 7. (*I*) qPCR analysis of Venus, *Oct4*, *Nanog*, *Sox2*, and *Rex1* in EBs. Transcript levels were normalized to *Gapdh* levels. Data are the mean ± SD of one biological sample assayed in three independent experiments and represent the relative expression levels of indicated genes in EBs produced without inhibitors (○) or with PAC (■) at days 0, 3, and 7. (Scale bars: 100 μm.)

TgWW1 cell at passage 9, the single cell attached to the internal surface of the blastocyst (Fig. 3*D*). In an embryo day (E) 16.0 fetus gonad, germ cell differentiation was confirmed by the detection of Venus fluorescence (Fig. 3*E*).

To generate coat-color chimeras, TgWL1 cells were injected into Wistar blastocysts using the YPAC injection method. Eight of 23 coat-color chimeras were obtained from the TgWL1 cell line at passage 11 or 12 (Fig. 3*F Right* and Table 3). Without the YPAC injection method, a coat-color chimera was hardly generated despite the fact that the same cell line, TgWL1, was used at earlier passages 6–8 (Fig. 3*F Left* and Table 3). Only 1 male chimera of 44 pups was obtained, but the chimerism was very sparse (Fig. S4). The generation of coat-color chimeras was successful in all six cell lines (Table 3). Those from cell line TgWW1 or LL1 are shown in Fig. S5. After mating with male rats, germline transmission was accomplished in adult female chimeras derived from all six cell lines independent of rat strains (Fig. 3*G* and Table 3). Genotyping analysis indicated that the *Oct4*-Venus transgene of the ES cells (TgWL2) was transmitted to filial (F)1 germline offspring with an agouti coat color (Fig. 3*H*).

Generation of ES Cell-Derived Tg Rats. We proposed to generate ES cell-derived transgenic (esTg) rats harboring the *Oct4*-Venus transgene, which shows a correct Venus expression pattern similar to Oct4 protein (Fig. 2*D*). After introduction of the *Oct4*-Venus transgene containing the same *Oct4* promoter/enhancer region as used in the generation of the conventional transgenic (cvTg) rats, 15 Venus-positive colonies (LL2 line) were picked up. After two passages, silencing of Venus gene expression occurred in 13 of 15 clones, resulting in an apparent heterogeneity in the fluorescence of Venus-positive clones (Fig. 4*A*, arrowheads), whereas only 2 clones kept homogenous Venus fluorescence (Fig. 4*B*). Chimeric

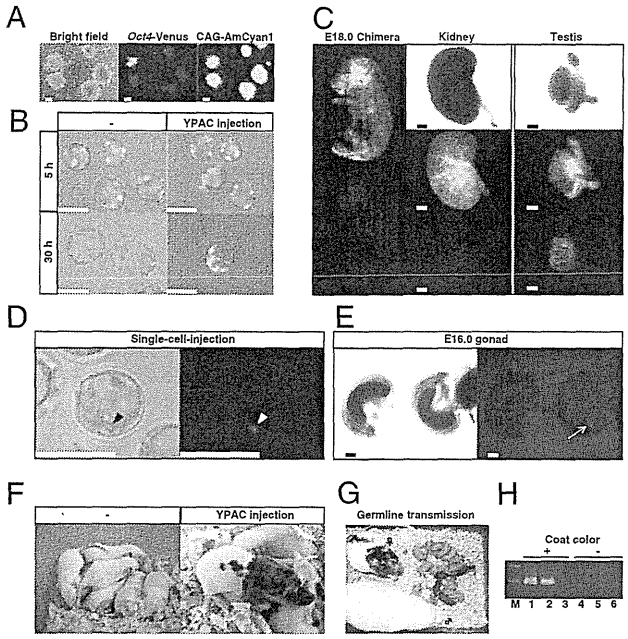

Fig. 3. Generation of germline chimeras by YPAC injection method. (*A*) Expression of AmCyan1 in stable transfectant clones (TgWW1 + C) generated by nucleofection with CAG-AmCyan1 plasmids. (*B*) Effect of YPAC during injection process. The basic ES cell medium with (*Right*) or without (*Left*) YPAC was used during the processes: injection of TgWW1 + C cells into blastocysts and incubation of the blastocysts for 30 h. (*C*) Generation of germline chimeras in embryos. TgWW1 + C cells were injected into Wistar blastocysts. Venus or AmCyan1 fluorescence was observed in E18.0 whole embryo, kidney, and testis. (*D* and *E*) Generation of germline chimeras by single-cell injection. (*D*) A single cell (TgWW1) was injected into a blastocyst. The image shows the injected blastocyst 3 h after incubation. The arrowhead indicates the injected single cell. (*E*) Venus-positive germ cells were detected in gonad at E16.0 (arrow). (*F*) Generation of coat-color chimeras by the YPAC injection. (*G*) Germline transmission in adult chimeras. The chimera (TgWL1) was mated with a Wistar male rat. Germline pups (4 of 16) were confirmed by an agouti coat color. (*H*) Genotyping analysis of F1 offspring of female chimera (TgWL2). The Venus region was amplified by PCR from genomic DNA of tail. M, 100-bp DNA marker; 1, 2, and 3, germline offspring with an agouti coat color; 4, 5, and 6, coat color-negative (albino) offspring. (Scale bars, *A*, *B*, and *D*: 100 μm; *C* and *E*: 300 μm.)

rats were produced via injection of the stable clone into Wistar blastocysts. Furthermore, germline transmission with the *Oct4*-Venus transgene was accomplished in the female chimeras (Fig. 4*C* and Table 3). The esTg embryos at 16.0 days postcoitum (dpc) exhibited Venus fluorescence in the gonads (Fig. 4*D*). The esTg rats were able to mature to adults without apparent abnormalities and had normal reproductive ability. We established ES cell lines from esTg blastocysts to confirm an expression pattern of Venus fluorescence. During outgrowth, their Venus expression pattern (Fig. 4*E*) was similar to that of cvTg blastocysts (Fig. 1*B*). However, long-passaged esTg cell lines (n = 3) maintained stable Venus expression in the ES cells (Fig. 4*F*). This result indicates our success in generating high-quality esTg rats possessing a correct expression pattern of Venus under the *Oct4* promoter/enhancer.

Discussion

Our results demonstrated that the use of a combination of serum and cell signaling inhibitors during outgrowth, cell culture, and blastocyst injection leads to the generation of germline chimeras with extremely high efficiency. Furthermore, we generated genetically modified rats from ES cells, termed esTg rats, growing up healthily and retaining reproductive ability. The advantage of this technology of using rat ES cells is that we can select Tg ES

Table 2. Summary of germline chimeras: Germ cell development in fetal gonad judged by Venus fluorescence

Cell line (gender)	Passage no.	Host blastocyst	Injected embryos	Fetal no.	Germline chimera
TgWL2 (XX)	6	LEA	43	9	1M1F
	22	Wistar	13	3	1F
		Wistar/LEA	23	9	1F
TgWW1 (XX)	6, 7	Wistar	53	9	2M7F
TgWW1 + C (XX)	8	Wistar	46	9	1M1M or F
TgWW1s (XX)	9	Wistar	35	8	1F
TgWW2* (XX)	8	Wistar	28	1	1M

F, female; M, male.
*ES cell line established by using specific serum. TgWW1 + C refers to a stable transfectant possessing CAG-AmCyan1 transgene.

cell clones that possess a correct gene expression pattern of the transgene. Our *Oct4*-Venus esTg rats will be useful for the generation of iPS cells as a pluripotency monitoring system with respect to previous work in mice (9, 18, 19). For further study, addressing the mechanism of the silencing effect on the transgenes should be crucial.

The complete generation of esTg rats might be based on the use of a culture medium containing 20% serum and YPAC, which might provide strong protectection from cell damage during gene introduction with electrical stimuli and maintain pluripotency with a stable karyotype during the cloning and expansion process. To support viability, serum was temporally used in a previous report when rat ES cells were electroporated and cultured overnight in a 2i medium (6). Such efforts are not necessary with our rat ES cells, which are tolerant to the damage induced by gene introduction because of the presence of 20% serum in the YPAC medium. Furthermore, we have confirmed that drug selection through the use of G418 is efficient in rat ES cells for generating genetically modified rats.

Previous work has suggested that the failure in the establishment of authentic rat ES cells over the past 2 decades was attributable to the presence of serum (6, 7). Indeed, serum may contain various kinds of nutrient factors as well as differentiation factors for rat ES cells (20). The reason why we succeeded in the establishment of such significant pluripotent cell lines might be attributable not only to the signaling inhibitors shielding ES cells from differentiation but to the use of the nutrients in the serum. Monitoring serum quality for better ES cell culturing is extremely important. Nevertheless, our combination of YPAC and different serum, which is used for culturing MEFs, allowed stable establishment of rat ES cell lines. Our success is thus partly attributable to the strong potential of YPAC in the maintenance of ES cells regardless of differentiation factors under different culture conditions.

It is noteworthy that leukemia inhibitory factor (LIF) was not necessary in our culture medium, although recent reports have suggested that its addition improved rat ES or rat iPS cell ability to suppress differentiation (6, 7, 10). It has been shown that LIF is the key cytokine secreted by feeders in supporting mouse ES cell self-renewal (21, 22) and that LIF was able to replace the requirement for feeders in propagation (23, 24). Ying et al. (8) demonstrated that a combination of PD0325901 and CHIR99021 enabled mouse ES cells to maintain pluripotency by substituting LIF, feeders, and serum. Considering these reports, the addition of LIF in our culture condition might be dispensable because of the inclusion of serum, MEFs, and the two inhibitors. Actually, the expression level of *Tbx3*, which is involved in mediating LIF signaling (25), was up-regulated in the rat ES cells. Moreover, we found that the expression of a suppressor of cytokine signaling 3 (*SOCS3*), which is one of the STAT3's direct target genes (26),

Table 3. Summary of germline chimeras: Chimeras and germline transmission judged by coat color of F1 pups

Cell line (gender)	Passage no.	Host blastocyst	Injected embryos	Pup no.	Chimera no.	Mating no.	Germline chimera
−YPAC injection							
TgWL1 (XX)	6–8	Wistar	226	44	1M*	0	—
+YPAC injection							
TgWL1 (XX)	11, 12	Wistar	123	23	3M5F	1M3F	1F
TgWL2 (XX)	4, 6	Wistar	70	10	2M3F	1M3F	2F
TgWW1 (XX)	9	Wistar/ LEA	79	19	5M3F	3F	1F
WW1 (XX)	10	LEA	27	7	2M1F	1F	1F
LL1 (XX)	4, 6	Wistar	107	13	3F	2F	1F
LL2 (XX)	9	Wistar	52	6	3F	3F	2F

F, female; M, male.
*Coat-color contribution is sparse (Fig. S5).

was up-regulated after stimulation with rat LIF (27) even in the YPAC medium. Thus, it seems possible to improve the culture condition further by the administration of rat LIF.

The six established ES cell lines in this work were all female. This result does not correspond to mice, because most of the mouse ES cell lines are male. In our present study, we continued to culture rat ES cell lines exhibiting rapid cell proliferation, resulting in the establishment of six female lines. Thus, we speculate that female blastocysts are suitable for the establishment of rat ES cells or that the addition of MEK and GSK3 inhibitors to the culture medium facilitates female-specific rapid cell growth in rat ES cells. A previous study using MEK and GSK3 inhibitors also reported that six of seven rat ES cell lines were female (6).

Although two groups reported the establishment of authentic rat ES cells, only one of several cell lines accomplished germline transmission in each group (6, 7). So far, there is no report of successful generation of knockout/knockin rats from ES cells. Thus, trials to produce more potent cell lines and to find the optimal combination of rat strains for donor ES cells, host blastocysts, and recipient foster female animals remain to be addressed (6, 7). In this study, our YPAC culture and injection method overcame the difficulty of completing germline transmission in all six ES cell lines independent of rat strains. The YPAC condition will enable the selection of preferable rat strains for the generation of genetically modified rats from ES cells, bringing great advantages to research for strain-specific disease models. We believe that the availability of our rat ES cells and the YPAC injection technique will also open up a valuable platform for routinely generating knockout/knockin rats, holding out the promise for generation of previously undescribed disease models.

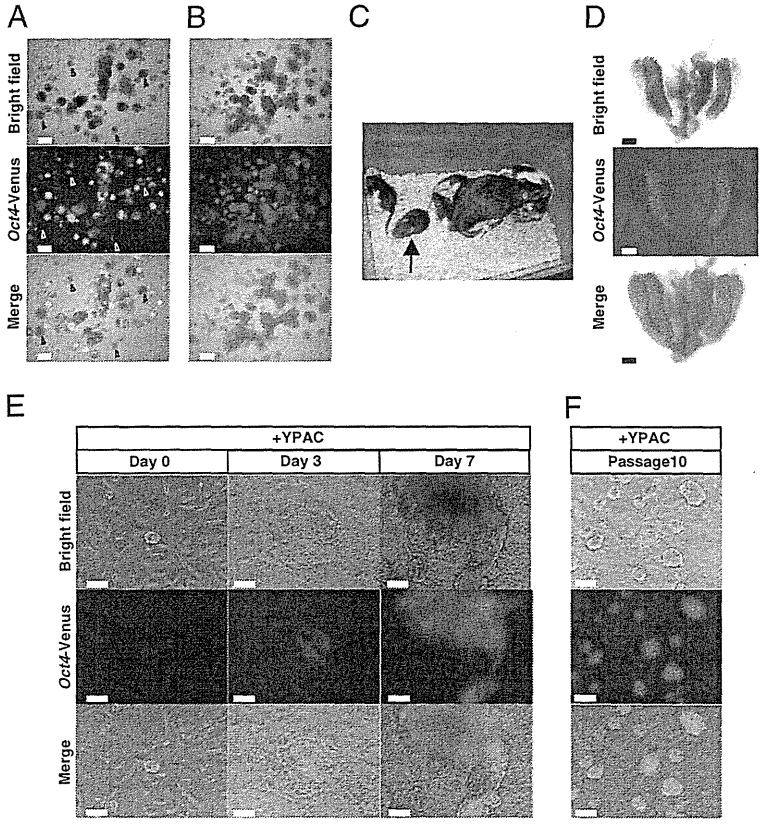

Fig. 4. Generation of Tg rats from ES cells. (*A* and *B*) Cloning and expansion of *Oct4*-Venus transfectants. An *Oct4*-Venus transgene was introduced into ES cells (LL2) at passage 5. Venus-positive clones were passaged without drug selection. (*A*) Arrowheads indicate ES cells with Venus expression silenced. (*B*) ES cells with homogeneous expression of *Oct4*-Venus. (*C*) Generation of Tg rats from ES cell clone displaying homogeneous expression of *Oct4*-Venus. An arrow indicates esTg rats through germline transmission from the chimeric rat. (*D*) Venus fluorescence in gonads of an esTg embryo at 16.0 days postcoitum (dpc). (*E*) Outgrowth of esTg blastocyst in YPAC medium. (*F*) Rat ES cell line derived from an esTg blastocyst. The expression of *Oct4*-Venus did not receive a silencing effect even after 10 passages. (Scale bars, *A*, *B*, and *D*: 300 μm; *E* and *F*: 100 μm.)

DEVELOPMENTAL BIOLOGY

Materials and Methods

Media, Feeder, Animals, and Primers. YPAC medium was prepared by the addition of the four respective inhibitors [10 μM Y-27632 (WAKO), 1 μM PD0325901 (Axon Medchem), 0.5 μM A-83-01 (TOCRIS), and 3 μM CHIR99021 (Axon Medchem)] to basic medium. The basic medium is composed of DMEM [including 110 mg/L sodium pyruvate and 200 mM GlutaMAX (GIBCO)], 20% (vol/vol) FBS (ES Cell Qualified FBS, Lot No. 1204059; GIBCO), 0.1 mM 2-mercaptoethanol (SIGMA), 1% nonessential amino acid stock (GIBCO), and 1× antibiotic antimycotic (GIBCO). Mitomycin C-treated MEFs resistant to neomycin (Millipore) were used as feeders and maintained in DMEM/10% (vol/vol) FBS (Lot No. SFB30-1502; EQUITECH-BIO, Inc.) medium with 1× antibiotic antimycotic. Animal experiments were performed in compliance with the guidelines of the Institute for Laboratory Animal Research, National Cancer Center Research Institute. The Wistar strain, LEA strain, or a hybrid of the Wistar and LEA strain was used in this work. All the primer sequences are listed in Table S1.

Generation of *Oct4*-Venus Tg Rats via a Conventional Method. The DNA fragment of the *Oct4* promoter region (3.9 kb) was obtained by PCR using KOD Version 2 DNA polymerase (Toyobo) from Wistar rat genomic DNA and was inserted into a pCS2-Venus plasmid (14). The *Oct4* promoter-Venus (*Oct4*-Venus) DNA fragment was injected into pronuclei of fertilized eggs in a Wistar rat strain (Oriental Yeast Co., Ltd.). Six Tg-positive founders were obtained from 222 injected fertilized eggs.

Establishment of Rat ES Cells from Blastocysts. Rat blastocysts were gently flushed out from the uteri of E4.5- or E5.0-timed pregnant rats with basic ES medium. After removal of the zona with acid Tyrode's solution (Ark Resource Co., Ltd.), whole blastocysts were plated onto six-well plates and cultured on MEFs in the basic ES medium with or without YPAC. After around 7 d, the blastocyst outgrowths were cut into pieces and replated under the same YPAC conditions. Emerging ES cell colonies were then dissociated using Accutase and were expanded. Established ES cell lines were routinely maintained under MEF-YPAC conditions and passaged every 3–4 d. Floated colonies were also passaged. Cells were cryopreserved and recovered by conventional procedures using YPAC medium and DMSO as a cryoprotectant. In the cell line of TgWL1 or TgWL2, 1,000 U/mL rat LIF (25) was added to the YPAC medium until passage 4 or 3, respectively.

Quantitative PCR Analysis. Total RNA was isolated using ISOGEN (Nippongene). cDNA was synthesized with 2 μg of the total RNA using Super Script III RT (Invitrogen) and oligo-dT primer (Invitrogen). cDNAs were used for PCR utilizing Platinum SYBR Green qPCR SuperMix UDG (Invitrogen). Optimization of the quantitative (q)RT-PCR was performed according to the manufacturer's instructions (PE Applied Biosystems). All quantitations were normalized to an endogenous control *GAPDH*.

ALP and Immunofluorescent Staining. Cells were fixed in 4% (wt/vol) paraformaldehyde. ALP staining was performed with Vector Blue substrate (Vector Labs) according to the manufacturer's instructions. Primary antibodies used include the following: Oct4 (C-10, 1:20; Santa Cruz), Nanog (1:20; ReproCell), and Sox2 (1:20; BioLegend). Alexa Fluor fluorescent secondary antibodies (Invitrogen) were used at a 1:500 dilution. Nuclei were visualized with DAPI staining.

Teratoma Formation. The 2.6×10^6 TgWW1 cells (passage 5) were injected under the skin of immunodeficient mice. Teratomas were obtained 34 d after the injection. They were embedded in paraffin wax and stained with H&E.

EB Formation. After ES cells were split into single cells using Accutase, they were cultured in a basal ES medium with or without three-inhibitor PAC, excluding Y-27632, on a low-cell-binding dish (NUNC). RNAs were extracted from the EBs at day 3 or 7, followed by qPCR examination.

Blastocyst Injection. The blastocysts from E4.5-timed pregnant rats were placed into 500 μL of injection medium composed of YPAC (or PAC) and basal ES cell medium without antibiotic antimycotic, and they were then incubated for 2–3 h. The well-expanded blastocysts were used for microinjection. For ES cell preparation, 10–20 domed or floated colonies were picked up by hand-made capillary and treated with an Accutase droplet for 5 min, followed by being split into single cells in a droplet of injection medium. The cells were transferred in 500 μL of the injection medium and incubated for 30–60 min at room temperature. After centrifugation, ES cells were transferred into a droplet of the injection medium under mineral oil (SIGMA). Ten to 15 ES cells were injected into each blastocyst and incubated at 37 °C for 3–5 h in the injection medium to allow the recovery of embryos. Ten to 20 embryos were then transferred into the uterine horn of each E3.5-timed pseudopregnant female rat. Chimeric rats were identified by coat color. Germline transmission was confirmed by the F1 rat coat color resulting from mating of chimera or *Oct4*-Venus fluorescence in germ cells in the fetal gonad. Genotyping of animals was carried out by PCR on tail DNA.

Gene Transfection of Rat ES Cells. For nucleofection, 5 μg of CAG-AmCyan1 or 10 μg of *Oct4*-Venus plasmid linearized by SalI was transfected into 3.2×10^6 TgWW1 or 3×10^6 LL2 rat ES cells, respectively, using a Mouse ES Cell Nucleofector Kit (Amaxa, Inc.). The cells were plated on MEFs in the YPAC medium with 2% (vol/vol) matrigel (BD Biosciences). Three combined colonies of CAG-AmCyan1 or a single colony of *Oct4*-Venus transfectant, positive for cyan or green fluorescence, respectively, was picked up by hand-made capillary and expanded without drug selection.

ACKNOWLEDGMENTS. We thank Shinobu Ueda, Takumi Teratani, Yoshitaka Tamai, and Taku Shimizu for technical advice; Luc Gailhouste for comments on the manuscript; Atsushi Miyawaki (RIKEN) for pCSII-Venus plasmid; Katsuyuki Hayashi and DNA Chip Research, Inc., for microarray analysis; and Setsuo Hirohashi and Masaaki Terada for great support of our project. This work was supported by a Grant-in-Aid for the Third-Term Comprehensive 10-Year Strategy for Cancer Control.

1. Jacob HJ (1999) Functional genomics and rat models. *Genome Res* 9:1013–1016.
2. Liao J, et al. (2009) Generation of induced pluripotent stem cell lines from adult rat cells. *Cell Stem Cell* 4:11–15.
3. Iannaccone PM, Jacob HJ (2009) Rats!. *Dis Model Mech* 2:206–210.
4. Geurts AM, et al. (2009) Knockout rats via embryo microinjection of zinc-finger nucleases. *Science* 325:433.
5. Ueda S, et al. (2008) Establishment of rat embryonic stem cells and making of chimera rats. *PLoS ONE* 3:e2800.
6. Buehr M, et al. (2008) Capture of authentic embryonic stem cells from rat blastocysts. *Cell* 135:1287–1298.
7. Li P, et al. (2008) Germline competent embryonic stem cells derived from rat blastocysts. *Cell* 135:1299–1310.
8. Ying QL, et al. (2008) The ground state of embryonic stem cell self-renewal. *Nature* 453:519–523.
9. Silva J, et al. (2008) Promotion of reprogramming to ground state pluripotency by signal inhibition. *PLoS Biol* 6:e253.
10. Li W, et al. (2009) Generation of rat and human induced pluripotent stem cells by combining genetic reprogramming and chemical inhibitors. *Cell Stem Cell* 4:16–19.
11. Lin TA, et al. (2009) A chemical platform for improved induction of human iPSCs. *Nat Methods* 6:805–808.
12. Ishizaki T, et al. (2000) Pharmacological properties of Y-27632, a specific inhibitor of rho-associated kinases. *Mol Pharmacol* 57:976–983.
13. Watanabe K, et al. (2007) A ROCK inhibitor permits survival of dissociated human embryonic stem cells. *Nat Biotechnol* 25:681–686.
14. Nagai T, et al. (2002) A variant of yellow fluorescent protein with fast and efficient maturation for cell-biological applications. *Nat Biotechnol* 20:87–90.
15. Chew JL, et al. (2005) Reciprocal transcriptional regulation of Pou5f1 and Sox2 via the Oct4/Sox2 complex in embryonic stem cells. *Mol Cell Biol* 25:6031–6046.
16. Yeom YI, et al. (1996) Germline regulatory element of Oct-4 specific for the totipotent cycle of embryonal cells. *Development* 122:881–894.
17. Keller GM (1995) In vitro differentiation of embryonic stem cells. *Curr Opin Cell Biol* 7:862–869.
18. Huangfu D, et al. (2008) Induction of pluripotent stem cells by defined factors is greatly improved by small-molecule compounds. *Nat Biotechnol* 26:795–797.
19. Esteban MA, et al. (2010) Vitamin C enhances the generation of mouse and human induced pluripotent stem cells. *Cell Stem Cell* 6:71–79.
20. Kawamata M, Ochiya T (2010) Establishment of embryonic stem cells from rat blastocysts. *Methods Mol Biol* 597:169–177.
21. Evans MJ, Kaufman MH (1981) Establishment in culture of pluripotential cells from mouse embryos. *Nature* 292:154–156.
22. Martin GR (1981) Isolation of a pluripotent cell line from early mouse embryos cultured in medium conditioned by teratocarcinoma stem cells. *Proc Natl Acad Sci USA* 78:7634–7638.
23. Smith AG, et al. (1988) Inhibition of pluripotential embryonic stem cell differentiation by purified polypeptides. *Nature* 336:688–690.
24. Williams RL, et al. (1988) Myeloid leukaemia inhibitory factor maintains the developmental potential of embryonic stem cells. *Nature* 336:684–687.
25. Niwa H, Ogawa K, Shimosato D, Adachi K (2009) A parallel circuit of LIF signalling pathways maintains pluripotency of mouse ES cells. *Nature* 460:118–122.
26. Burdon T, Chambers I, Stracey C, Niwa H, Smith A (1999) Signaling mechanisms regulating self-renewal and differentiation of pluripotent embryonic stem cells. *Cells Tissues Organs* 165:131–143.
27. Takahama Y, et al. (1998) Molecular cloning and functional analysis of cDNA encoding a rat leukemia inhibitory factor: Towards generation of pluripotent rat embryonic stem cells. *Oncogene* 16:3189–3196.